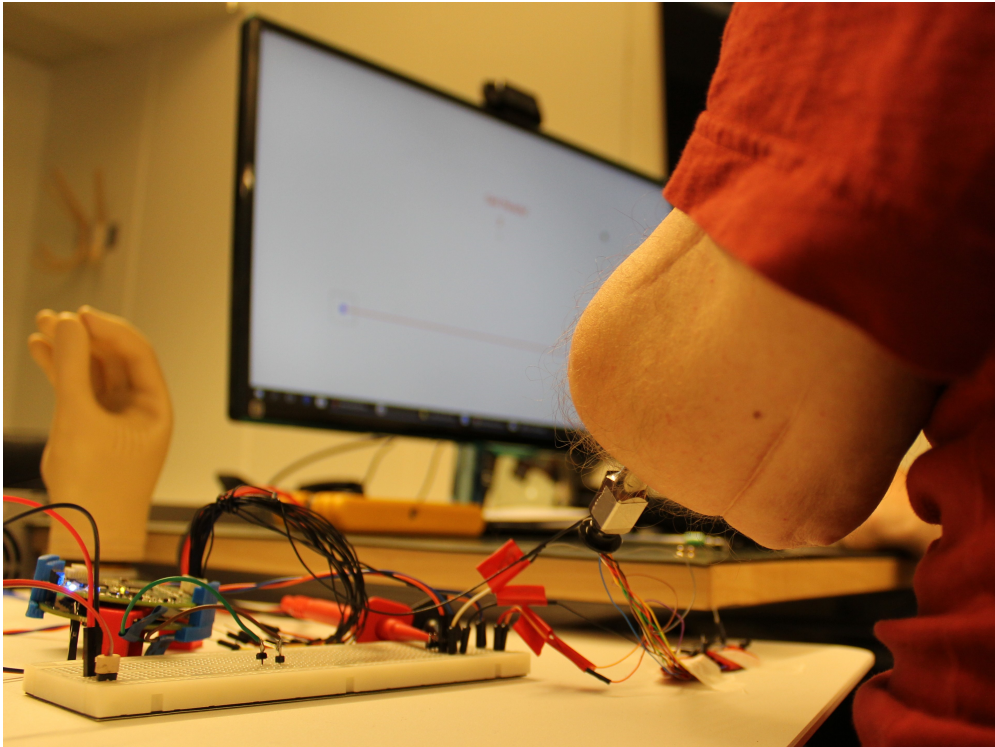




CHALMERS
UNIVERSITY OF TECHNOLOGY



Direct Stimulation of Peripheral Nerves to Provide Sensory Feedback

Master's thesis in Biomedical Engineering

Clara Günter

MASTER'S THESIS 2019

Direct Stimulation of Peripheral Nerves to Provide Sensory Feedback

CLARA GÜNTER



CHALMERS
UNIVERSITY OF TECHNOLOGY

Department of Electrical Engineering
Biomedical Signals and Systems
Biomechatronics and Neurorehabilitation Laboratory
CHALMERS UNIVERSITY OF TECHNOLOGY
Gothenburg, Sweden 2019

Direct Stimulation of Peripheral Nerves to Provide Sensory Feedback
CLARA GÜNTER

© CLARA GÜNTER, 2019.

Supervisor/Examiner: Max Ortiz-Catalan, Department of Electrical Engineering

Master's Thesis 2019
Department of Electrical Engineering
Biomedical Signals and Systems
Biomechatronics and Neurorehabilitation Laboratory
Chalmers University of Technology
SE-412 96 Gothenburg
Telephone +46 31 772 1000

Cover: subject with osseointegrated abutment during an experiment.

Typeset in L^AT_EX
Printed by [Name of printing company]
Gothenburg, Sweden 2019

Acknowledgements

There is a number of people without whom the extent of this thesis would not have been manageable, therefore, I would like to thank:

- My supervisor Max Ortiz-Catalan for giving me the opportunity to work on this project, and presenting a part of it at an international conference.
- Jean Delbeke and Max Ortiz-Catalan for their co-authorship of the literature review.
- Jon Sensinger for his valuable advice in setting up the methodology for this study.
- All members of the Biomechatronics and Neurorehabilitation Laboratory at Chalmers, especially Enzo and Jan, for helping out whenever they could and numerous lunchtime and Fika discussions.
- Everyone who "volunteered" as a subject.
- My family, especially my mum, for helping me in any way possible and allowing me to come to Sweden for this last part of my studies.

Clara Günter, Gothenburg, January 2019

Contents

List of Figures	ix
List of Tables	xi
Preface	1
1 Assessment of Internal Model Strength based on augmented feedback	3
Introduction	3
1.1 Introduction	4
1.2 Methods	7
1.2.1 Task Description	7
1.2.2 Equipment	7
1.2.3 Control	9
1.2.4 Feedback	9
1.2.4.1 Visual Feedback	10
1.2.4.2 Sensory Feedback by electrical stimulation of peripheral nerves	10
1.2.4.3 Augmented Feedback	10
1.2.5 Familiarization	10
1.2.6 Outcome Measures	11
1.2.6.1 Adaptation Rate	11
1.2.7 Just-noticeable Difference	11
1.2.8 Experiment Layout	12
1.2.9 Experiment A: Able-bodied Subjects	12
1.2.10 Experiment B: Case Study with one Amputee Subject	12
1.3 Results	13
1.3.1 Experiment A	13
1.3.1.1 Validation and Adaptation of Task Parameters	13
1.3.1.2 Frame of Reference for Outcome Values	15
1.3.2 Experiment B	16
1.3.2.1 Stimulation Parameters	16
1.3.2.2 Augmented feedback and different modulation paradigms	19
1.3.2.3 Comparison of Outcome Parameters Experiment A versus Experiment B	22

1.4	Discussion	23
1.4.1	Task Parameters	23
1.4.2	EMG Control	23
1.4.3	Latency	24
1.4.4	Sensory feedback by electrical stimulation of peripheral nerves	24
1.4.5	Feedback Modalities	24
1.4.6	Limitations	25
1.5	Conclusion	26
1.6	Outlook	26
	References	26
2	Safety of long-term electrical peripheral nerve stimulation	31

List of Figures

1.1.1 Schematic view of the motor learning process for able-bodied subjects. A motor command from the central nervous system (CNS), is, with the help of parameters estimated the internal model, transferred through the peripheral nervous system (PNS) to muscle activity and thus results in an alteration in limb position. A feedforward command is sent and updated offline (a) after the completion of the intended movement, by the feedback controller (predictive control). Further, feedback is used in online correction (b) of a movement (reactive control).	5
1.1.2 Schematic view of the motor learning process for amputee subjects. A motor command from the central nervous system (CNS), is, with the help of parameters estimated the internal model, transferred through the peripheral nervous system (PNS) to muscle activity. These signals are recorded with electrodes and fed into the prosthesis control algorithm which then controls prosthetic limb position. A feedforward command is sent and updated offline (a) after the completion of the intended movement, by the feedback controller (predictive control). Further, feedback is used in online correction (b) of a movement (reactive control).	6
1.2.1 Experiment setup.	8
1.2.2 Screenshot of task. Arrows indicate starting position, cursor that is controlled by the subject, target, and ideal movement progression. . .	9
1.3.1 Evolution of error magnitude for able-bodied subjects over one block of 70 trials. The shaded region shows the standard deviation of error value of all subjects for each trial, the curve shows the mean error of all subjects for each trial with a moving average filter (size = 5). . . .	14
1.3.2 Evolution of JND for able-bodied subjects over one block with 25 reversals. Variations over reversals are calculated by subtracting JND after 25th reversal from JND after respective reversal.	14
1.3.3 Adaptation rates for able-bodied subjects calculated with different cutoff points. Median values are $5.7 \cdot 10^{-3}$ for cutoff at 30, $7.5 \cdot 10^{-3}$ for cutoff at 40, $7.2 \cdot 10^{-3}$ for cutoff at 50, $5.8 \cdot 10^{-3}$ for cutoff at 60, and $4.1 \cdot 10^{-3}$ for cutoff at 70 trials. Boxplot midline represents the median, edges of each box show the 25 th and 75 th percentile. Outliers are noted by a '+'.	15

1.3.4 Just-noticeable differences for able-bodied subjects after 20 and 25 reversals. Median values are 53.6% after 20 reversals and 50.0% after 25 reversals. Boxplot midline represents the median, edges of each box show the 25th and 75th percentile. Outliers are noted by a '+'. 16

1.3.5 Location of sensation for different pulse widths (blue = 200 μ s, red = 400 μ s, green = 500 μ s). I = 400 μ A; F = 25Hz; N= 2. The 200 μ s pulses were perceived in a small, refined area. The 400 μ s pulses were perceived in a larger area along the thumb. The 500 μ s pulses were perceived first to a small area near the wrist and then moved up towards the thumb. The intensity of perception was identical for pulse pairs with 200 μ s and 400 μ s duration but increased for pulse pairs with 500 μ s duration (see Table 1.3.2a). 17

1.3.6 Location of sensation for different pulse amplitudes (blue = 390 μ A, red = 450 μ A, green = 500 μ A). W = 200 μ s; F = 25Hz; N = 2. All pulse pairs of different amplitude were perceived in the same refined location, only intensity of the perception increased (see Table 1.3.2b). 18

1.3.7 Evolution of error magnitude for different feedback conditions for amputee subject over one block of 70 trials. Errors are filtered with a moving average filter (size=5). The upper plot shows feedback conditions including visual feedback. The lower plot shows feedback condition excluding visual feedback. 20

1.3.8 Conventional adaptation rate and absolute errors for different feedback conditions over 50 trials by amputee subject. Adaptation rates are $2.3 \cdot 10^{-3}$ for VSA, $1.5 \cdot 10^{-3}$ for SA, $5.7 \cdot 10^{-3}$ for VSW, $0.9 \cdot 10^{-3}$ for SW, and $4.4 \cdot 10^{-3}$ for V. 21

1.3.9 Just-noticeable difference after 20 reversals for different feedback conditions by amputee subject. Just-noticeable differences are 17.2% for VSA, 25.1% for SA, 84.3% for VSW, 85.7% for SW, and 66.1% for V. 22

List of Tables

1.2.1 Test Block Layout.	12
1.2.2 Order of Feedback conditions presented to subject in experiment B. . .	13
1.3.1 Stimulation Parameters.	17
1.3.2 Perceived intensities for different parameters.	18

Preface

For a long time, the field of prosthetics has focused mostly on improving control algorithms. Aspects of feedback in prosthetics have been discussed, however, no single method has yet emerged as optimal solution. Emerging technologies allow for near-natural ways to provide feedback, such as by electrical neurostimulation. Although first promising results have been obtained, thorough examination and quantification of presumed improvements are lacking. Furthermore, there is limited availability of literature on safety regulations and guidelines required for chronic electrical neurostimulation.

In this thesis, two issues in direct stimulation of peripheral nerves are discussed:

1. the effect of feedback by electrical stimulation of peripheral nerves on internal model strength, and
2. the safety of long-term electrical peripheral nerve stimulation.

1

Assessment of Internal Model Strength based on augmented feedback

Abstract

Augmented feedback by electrical stimulation of peripheral nerves and the method of pulse modulation have not yet been evaluated in a quantifiable manner. A simple test paradigm may allow for quantification of internal model strength and thus of efficiency of feedback modes.

A test paradigm developed to examine quality of feedback in a rehabilitation was expanded to EMG control. Each experimental session consisted of an adaptation rate test and a just-noticeable difference test. Two experiments were conducted. In experiment A, eight able-bodied subjects completed the experiment in order to show viability of the test with EMG control, to provide knowledge about number of trials and reversals required for the two tests and to provide a frame of reference for ranges in outcome measures. In experiment B one amputee subject completed five feedback conditions were completed, namely: visual, sensory by amplitude modulated pulses, sensory by width modulated pulses, augmented (visual and sensory by amplitude modulated pulses), augmented (visual and sensory by width modulated pulses).

In experiment A both outcome measures (adaptation rate and just-noticeable difference) showed clear convergence until trial 40 and reversal 22, thus showing viability of EMG control. A frame of reference was established. In the case-study in experiment B, adaption rates showed no clear trend. Just-noticeable differences, however, showed improved scores for augmented feedback with sensory feedback by amplitude modulated pulses.

Despite some flaws in experiment design, promising results were obtained. Analyzing the two tests, adaptation rate as it is currently calculated may not be a good indicator of internal model strength. If low error magnitude was reached early on, the adaptation rate did not depict this. Just-noticeable differences for able-bodied subjects as well as the amputee subject seemed to provide a better estimation of how well the task was learned. To provide a better insight, several parameters of the experiment must be improved. This includes using a more adequate sampling rate for EMG and a reduction of trial numbers.

1.1 Introduction

Despite recent advances in the field of prosthetics, functionality of bionic limbs is still far from being near-natural. A feature that could potentially increase prosthetic function is augmented feedback. Sensory feedback by electrical stimulation of peripheral nerves is intuitive for the user and reduces the need for additional cognitive efforts. Augmented feedback in prostheses has been proven to enhance performance in grasping tasks under uncertainty [1], but the effect was observed to be limited once a task has been learned [2]. A possible reason for these ambiguous outcomes is explained by the concept of the internal model used to describe processes of motor learning [3].

The principle of internal models originates in control theory and was first introduced by Francis and Wonham in 1976 [4]. The theory was later extended to motor control and motor learning [5]. The internal model is hypothesized to be an inverse model of the system dynamics that serves to improve motor control [6]. Motor learning, and therefore also quality of the internal model, is based on three classes of control [3]:

1. predictive (feedforward) control;
2. reactive (feedback) control; and
3. biomechanical control.

Feedback is thought to play a major role in the formation, maintenance, and adaptation of one's internal model [7]. Therefore, augmented feedback should improve the internal model strength and thus also the long-term motor performance of a prosthetic user [8].

For able-bodied subjects, the internal model can schematically be visualized as seen in Figure (1.1.1). A motor command from the central nervous system (CNS) is, with the help of parameters estimated with the internal model, transferred throughout the peripheral nervous system (PNS) to muscle activity, and thus results in an alteration in limb position. A feedforward command is sent and updated offline after the completion of the intended movement, by the feedback controller (predictive control, see Figure 1.1.1). Further, feedback is used in the online correction of a movement (reactive control, see Figure 1.1.1). Biomechanical control, including aspects such as limb stiffness and impedance control, is an important component of motor control in able-bodied subjects, and serves to counteract effects of noise [9].

In able-bodied subjects, an internal direct mapping between input (i.e. the motor command) and output (i.e. limb position) exists. However, for amputee subjects controlling a prosthesis, an additional component is added to the schematic: the prosthesis control algorithm (see Figure 1.1.2). Due to this additional component, it is difficult to quantify internal model strength with the help of reaching or grasping tasks, as often used in able-bodied subjects. Therefore, an isolation of the internal model component is desirable to quantify any changes in the internal model in amputees. Artificial biomechanical control has, up to date, not been implemented in prostheses. As indicated in Figure (1.1.2), visual and tactile feedback were consid-

ered, and proprioceptive feedback was neglected. This restriction is due to the fact that proprioceptive feedback has only recently been implemented for amputees [10].

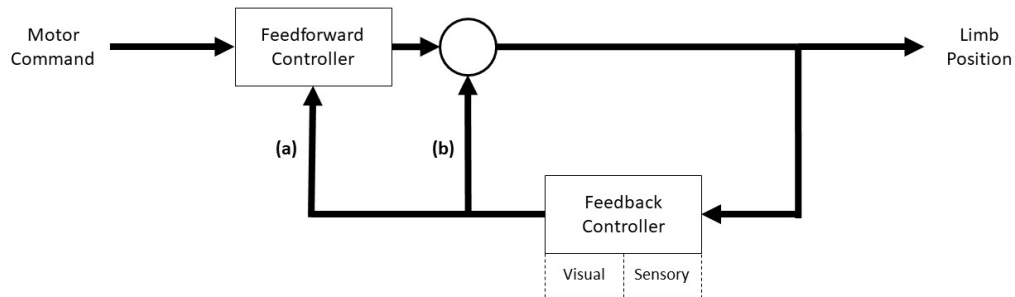


Figure 1.1.1: Schematic view of the motor learning process for able-bodied subjects. A motor command from the central nervous system (CNS), is, with the help of parameters estimated the internal model, transferred through the peripheral nervous system (PNS) to muscle activity and thus results in an alteration in limb position. A feedforward command is sent and updated offline (a) after the completion of the intended movement, by the feedback controller (predictive control). Further, feedback is used in online correction (b) of a movement (reactive control).

In rehabilitation and disabled subjects, knowledge of mechanisms of sensorimotor learning is required to improve the quality and duration of (re)learning motor skills. Radhakrishnan et al. [11] investigated learning of various EMG controlled interfaces. They showed that learning of intuitive as well as non-intuitive control interfaces was possible and concluded that the motor system could adapt any transformation by learning the inverse model of a control interface. In their study, task performance was impaired by introducing noise into the feedback, however, learning still occurred. Körding and Wolpert [12] described the use of Bayesian integration in sensorimotor learning, by showing that feedback uncertainty and distribution of a perturbation were included in the internal representation of a task. Therefore, learning control of an EMG controlled interface can be both hindered or assisted by varying feedback conditions.

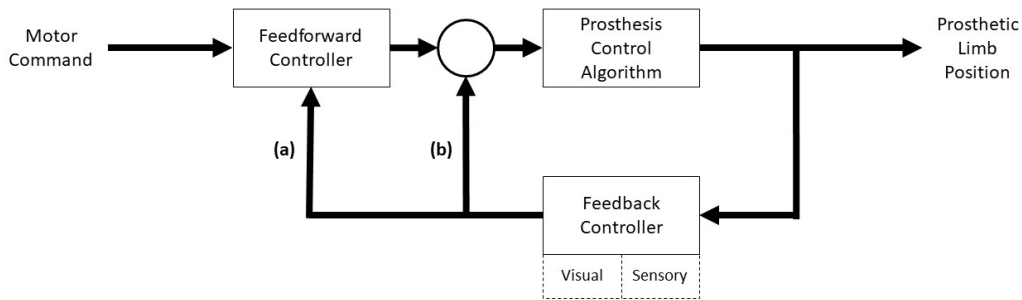


Figure 1.1.2: Schematic view of the motor learning process for amputee subjects. A motor command from the central nervous system (CNS), is, with the help of parameters estimated the internal model, transferred through the peripheral nervous system (PNS) to muscle activity. These signals are recorded with electrodes and fed into the prosthesis control algorithm which then controls prosthetic limb position. A feedforward command is sent and updated offline (a) after the completion of the intended movement, by the feedback controller (predictive control). Further, feedback is used in online correction (b) of a movement (reactive control).

Previous studies on the topic of internal model strength or performance level based on augmented feedback reached ambiguous conclusions about the effect and necessity of this feedback after an initial training period [1, 2, 7, 13, 14]. Schiefer et al. deemed augmented feedback to be helpful in the learning process but redundant after a task had been learned. Whereas Saunders and Vijayakumar argued that augmented feedback improved performance in the presence of uncertainty. Dosen et al. found a learning effect similar to that described in [1] to fade after some time. These outcomes can be explained by taking into account results from previous studies, that found regularly performed movements are performed relying mostly on the feedforward component of the internal model and feedback becomes somewhat redundant [13, 14]. Dosen et al. [7] showed that this effect of redundant feedback faded after a number of trials. Therefore, there was a necessity of augmented feedback to improve performance permanently when using an EMG control interface.

Resulting from the problematic evaluation of functional improvement based on feedback, objectively measuring differences between sensory feedback modalities is a challenging task. Encoding of electrical stimuli has proven to be difficult in the past [15–19]. The exact mechanisms for encoding location, quality and size of a sensation are mostly speculated upon. Therefore, the decoded stimulus sensation is often attributed to a feeling of paresthesia rather than ‘natural’ touch. Originally, only one parameter in the stimulation pulses was modulated, e.g. frequency, amplitude, and

width were changed one at a time (e.g. [20, 21]). More recently, Tan et al. developed a stimulation pulsing pattern, changing the stimulation pulse width within a 1Hz sinusoidal envelope and reported a ‘natural’ percept in two subjects. The method of pulse modulation most intuitive remains unknown at this point. Examining internal model strength with different modes of feedback could improve knowledge on this subject.

A test paradigm has been developed by Blustein and Sensinger [22], to examine the effect of feedback in a rehabilitation. The task consisted of a time-constrained reaching movement with a computer mouse while different modes of feedback (visual, audio, vibratory, combined) were provided. The outcome measures of this task allow for a quantification of internal model strength. To be used with amputees, this task must be expanded to EMG control and an intuitive mode of feedback. In summary, the aim of this work was threefold:

1. to expand Blustein and Sensinger’s task to EMG control and augmented feedback by electrical stimulation of peripheral nerves;
2. to quantify the value of feedback by electrical stimulation of peripheral nerves, and
3. to identify which method of modulation of such electrical stimulation is optimal for the prosthetic user.

1.2 Methods

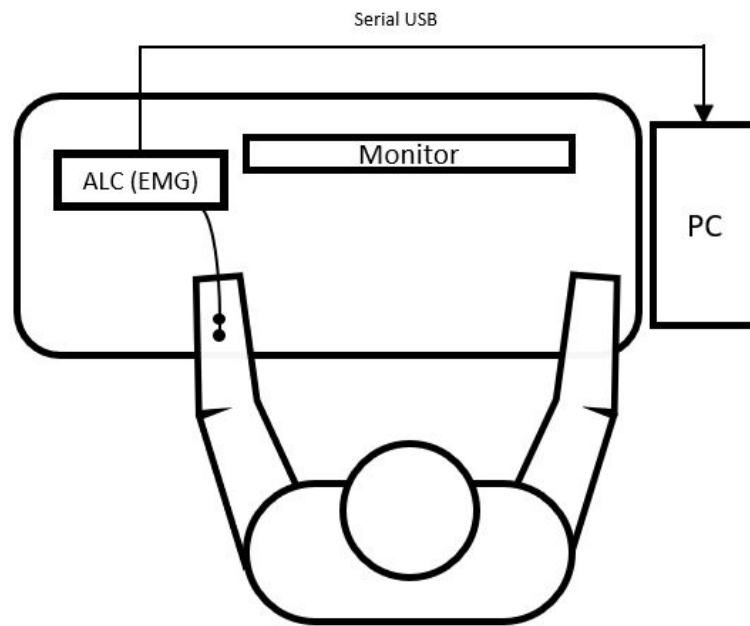
A task developed to examine rehabilitation outcome based on feedback developed by Blustein and Sensinger [22], was extended to EMG control and feedback by electrical stimulation of peripheral nerves. The effect of augmented and limited feedback as well as the method of pulse modulation on performance in this task was examined.

1.2.1 Task Description

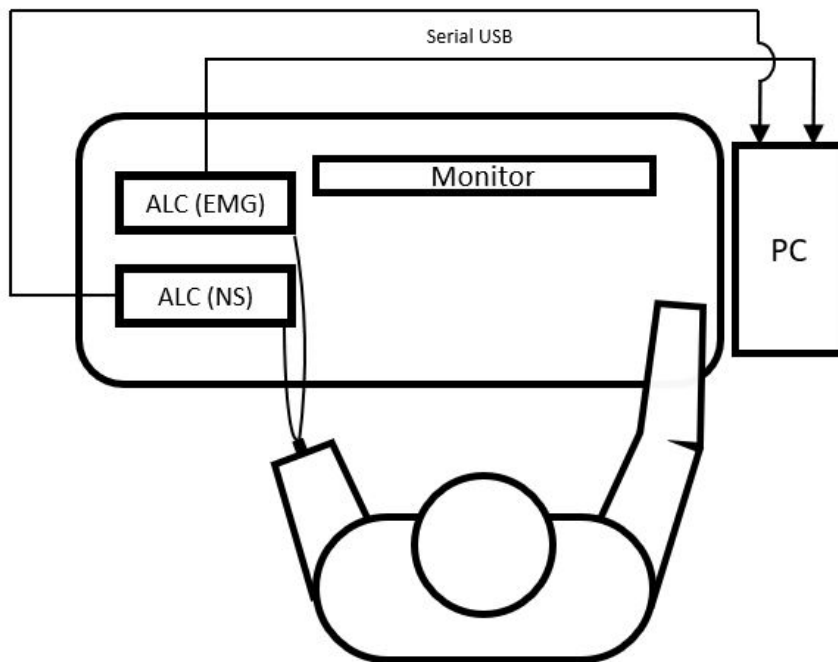
The test consisted of a time-constrained, movement task as suggested by Blustein and Sensinger [22]. The task objective was to move a cursor from the left to the right side of the screen within a defined period of time ($0.28 \text{ s} < t < 1.16 \text{ s}$, adapted from [22]). If the task was not completed within this interval, the trial was classified as unsuccessful and repeated until the requisites were met. The optimal movement timing was indicated by a second cursor located on the right side of the screen, moving vertically towards the same target area. This optimal movement cursor started moving 400 ms before the beginning of each trial. Trial start was indicated by the optimal movement cursor crossing a starting line. The experimental setup and a screenshot of the completed task can be seen in Figures 1.2.1 and 1.2.2, respectively.

1.2.2 Equipment

The artificial limb controller (ALC) [23], used to acquire EMG and perform neurostimulation, was connected via serial USB to a PC. All tasks were programmed in



(a) Experiment setup for able-bodied subjects. One EMG-channel (surface electrodes) recorded with the artificial limb controller (ALC) is used for control, visual feedback is provided via the monitor.



(b) Experiment setup for amputee subject. One EMG channel (implanted electrodes) recorded with the artificial limb controller (ALC) is used for control. Feedback is provided visually (monitor) and via electrical peripheral nerve stimulation (NS) via the artificial limb controller (ALC).

Figure 1.2.1: Experiment setup.

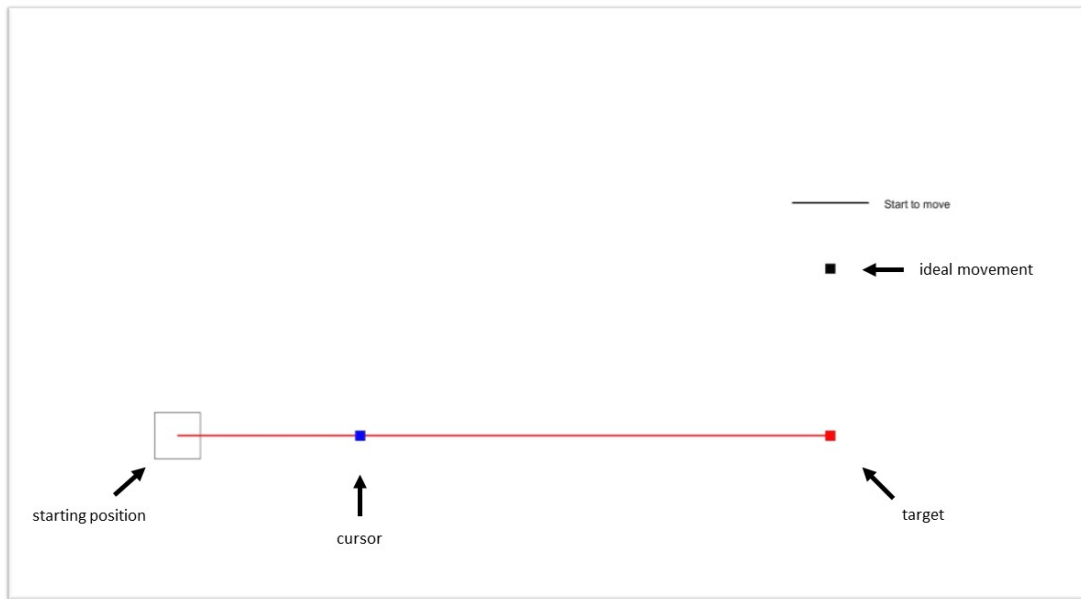


Figure 1.2.2: Screenshot of task. Arrows indicate starting position, cursor that is controlled by the subject, target, and ideal movement progression.

MATLAB (Ver. 2016b, The Mathworks, Inc. Natick, MA, USA). The task screen was displayed on a 27-inch computer monitor placed approximately 80 cm from the subject.

1.2.3 Control

The cursor in this task (see Figure 1.2.2) was controlled by a one channel EMG signal. The movement performed by subjects was ‘open hand’. The EMG signal was sampled at 250 Hz. Additional to an anti-aliasing filter implemented on the ALC (see [23]), a 50Hz notch filter and a 5Hz high pass filter were implemented in Matlab. The mean absolute (MABS) value of EMG was calculated for windows of 40 ms without overlap. Minimum and maximum thresholds were chosen by obtaining MABS values at rest and for maximum voluntary contraction. Proportional control was implemented within these defined thresholds and used to move the cursor in one direction. To test the adequacy of control thresholds, subjects were instructed to rest and perform maximum voluntary contraction. The requirement was no cursor movement for the first test and unsuccessful, ‘too fast’ trial for the latter (meaning $t < 0.28s$).

1.2.4 Feedback

Five different feedback conditions were tested, namely:

1. V - visual
2. VSA - visual and sensory (amplitude modulation)
3. SA - sensory (amplitude modulation)

4. VSW - visual and sensory (width modulation)
5. SW - sensory (width modulation)

1.2.4.1 Visual Feedback

Visual feedback was given in the form of a moving cursor (see Figure 1.2.2). The cursor position was updated at a rate of 25 Hz. If provided, visual feedback was given in the first 300 ms and at the endpoint of the task. This prevented an online correction of the movement; therefore, the provided feedback was only used to update the feedforward controller of the internal model and effects were limited to this component (see Figures 1.2.1a and 1.1.2).

1.2.4.2 Sensory Feedback by electrical stimulation of peripheral nerves

The amputee subject is implanted with a 3-contact self-sizing cuff nerve electrode (similar to [24]). The technology used for neurostimulation was described by Mastinu et al. [23]. One of these contacts was chosen for stimulation. Due to safety concerns [25], the contact with the lowest perception threshold was used, regardless of perceived location. Stimulation thresholds were determined at the beginning of the experimental session. Depending on feedback modality, the modulated parameter was increased proportionally to the cursor position with an update rate of 25 Hz. One stimulating pulse was sent for each update, resulting in a stimulation frequency of 25 Hz. Modulation of pulse width (SW) and pulse amplitude (SA) was used for encoding of information. If provided, sensory feedback was continuous.

Determination of stimulation parameters Previous to the beginning of the experiment the subject was asked about any phantom limb sensations. To determine the perception threshold for pulse amplitude and pulse width, the subject was presented with a two alternative forced choice test [26]. From perception threshold, each tested parameter was increased individually, first to 140 % of threshold, then with a step size of 10 μ s and 10 μ A, respectively, until the intensity of sensation was rated 7/10 by the subject or until the neurostimulator was saturated. The location and size of sensation were recorded by the subject by drawing on a sketch of a hand for minimum and maximum stimulation values, as well as an intermediate value.

1.2.4.3 Augmented Feedback

Augmented feedback consisted of a combination of the previously mentioned feedback modalities. Two augmented feedback conditions, namely ‘visual and sensory feedback with width modulated pulses (VSW)’ and ‘visual and sensory feedback with amplitude modulated pulses (VSA)’, were tested.

1.2.5 Familiarization

The initial familiarization phase consisted of oral instructions and a demonstration of a recording of the ideal movement of the cursor. Subsequently, the subject was able to familiarize themselves with the control and control parameters could be adapted

if needed. A brief familiarization phase of 2x5 successful trials was completed before each test block to familiarize the subject with the new feedback and test modality. The familiarization time was limited to 5 minutes or whenever the subject felt ready to advance to the test. After this initial phase, control and stimulation parameters were not altered throughout the test.

All familiarization trials were recorded for evaluation.

1.2.6 Outcome Measures

As described by Blustein and Sensinger [22], adaptation rate and just noticeable difference were used as outcome measures to quantify internal model strength.

1.2.6.1 Adaptation Rate

An adaptation rate test as suggested by [27] and [22] was performed. A number of 70 successful trials was performed, an increase in trials compared to [22] was deemed necessary to account for the increased complexity of EMG control versus control of a computer mouse. A subject's adaptation rate was then calculated with the equation:

$$error_{n+1} - error_n = \beta_1 \cdot error_n + \beta_0 \quad (1.2.1)$$

with $error_n$ equal to the error in seconds in trial n , $error_{n+1}$ equal to the error in seconds in trial $n + 1$, and the absolute value of β_1 equal to the adaptation rate.

1.2.7 Just-noticeable Difference

The just-noticeable difference for a specific task varies with different control and feedback modalities (as shown in e.g. [8]). A pair of two trials was presented, one of which was perturbed. The perturbation consisted of a displacement of the cursor in the positive direction introduced at $t = 300$ ms. This point in time was chosen over an initial displacement at $t = 0$ ms so that a displacement would not be clearly visible in feedback modalities including visual feedback. After completion of both trials, the subject was asked to indicate which trial they thought to be perturbed in a two alternative forced choice paradigm by choosing a field in a pop-up box. The magnitude of the perturbation was then updated with the equation:

$$x_{n+1} = x_n - \frac{c}{n_{shift} + 1} [correct_n - \Phi] \quad (1.2.2)$$

with x equal to the perturbation magnitude, c equal to the initial step size, n_{shift} equal to the number of reversals and Φ equal to the target probability, as introduced by Faes et al. [28]. c was set to two times the standard deviation of the error in the adaptation rate test and Φ was set to 0.84. The perturbation magnitude after 20 and 25 reversals, respectively, was used as just-noticeable difference.

1.2.8 Experiment Layout

The experiment was conducted in test blocks, each of which consisted of Familiarization, Adaptation Rate Test and Just-Noticeable Difference Test, in this order (see Table 1.2.1). The feedback modality was changed for each block. Feedback modalities as described before were: visual (V); sensory, pulse amplitude modulation (SA); sensory, pulse width modulation (SW); augmented pulse amplitude modulation (VSA); augmented pulse width modulation (VSW). The order of these test blocks was randomized, with ‘VSA’ and ‘SA’, and ‘VSW’ and ‘SW’ being grouped together. Total time for each block was around 45 minutes, with breaks of at least 15 minutes between blocks. Therefore, for all feedback conditions, the total experiment time added up to around 5 hours.

Test Block Layout
Familiarization
Adaptation Rate
Just-noticeable Difference

Table 1.2.1: Test Block Layout.

1.2.9 Experiment A: Able-bodied Subjects

The purpose of experiment A was threefold:

1. to show the viability of the task with EMG control,
2. to provide knowledge about the number of trials and reversals required for AR and JND test, respectively, and
3. to provide a frame of reference for ranges in outcome measures.

Eight right hand dominant, able-bodied subjects (4 male; Age: 25 ± 2 years) were recruited by convenience sample. All subjects were informed of the general purpose before the experiment and provided written consent the experiment. Two subjects had to be excluded from data analysis, due to administration errors. Data obtained from the remaining six subjects (4 male; Age: 26 ± 2 years) was used for analysis.

Common Ag/AgCl surface electrodes attached to the forearm of the subjects were used for control. The electrodes were attached to the extensor muscles of the posterior forearm, at around one-third of the forearm (measured from lateral epicondyle of the humerus to styloid process of the radius). The subjects completed the adaptation rate and the just-noticeable difference tests for the visual feedback condition. 70 successful trials and 25 reversals were required to complete the AR and JND test, respectively.

1.2.10 Experiment B: Case Study with one Amputee Subject

The purpose of experiment B was twofold:

1. to examine whether augmented feedback by electrical stimulation of peripheral nerves is beneficial in the formation of an internal model, and

Block Number	Feedback Condition
1	Visual and sensory feedback (amplitude modulation)
2	Sensory feedback (amplitude modulation)
3	Visual and sensory feedback (width modulation)
4	Sensory feedback (width modulation)
5	Visual feedback

Table 1.2.2: Order of Feedback conditions presented to subject in experiment B.

2. to gain knowledge about the pulse modulation technique that is more beneficial to the subject in achieving this.

One transhumeral amputee implanted with the osseointegrated human-machine gateway [24], consisting of epimysial electrodes for control and nerve cuff electrodes in median and ulnar nerves for feedback. The subject uses his prosthesis and an embedded system for acquisition of EMG and neurostimulation, or ALC [23], on an everyday basis. At the time of the experiment, neurostimulation had only been applied in a lab environment. The subject was informed of the general purpose and provided written consent before the experiment. Ethical approval was given the regional ethical committee.

An implanted epimysial electrode on a muscle reinnervated to respond to hand opening was used to control the cursor.

The subject completed AR and JND tests for five feedback conditions, the order of which is visualized in Table 1.2.2. The AR and JND tests were carried out until 70 successful trials and 20 reversals were reached, respectively. Stimulation Parameters are reported according to the parameters suggested in [25].

1.3 Results

This study examined internal model strength based on a test suggested by Blustein and Sensinger [22], with an EMG control interface. An adaptation rate test and a just-noticeable difference test was performed by six able-bodied subjects with visual feedback (Experiment A), and by one amputee subject with five different feedback conditions (Experiment B).

1.3.1 Experiment A

1.3.1.1 Validation and Adaptation of Task Parameters

The evolution of errors in the AR test shows a steady decrease in mean and standard deviation over trials 1 to 40, marginal changes in mean and standard deviation over trials 40 to 60 ($30\text{ms} \pm 70\text{ms}$), and an increase in both values is observed after trial 60 (see Figure 1.3.1).

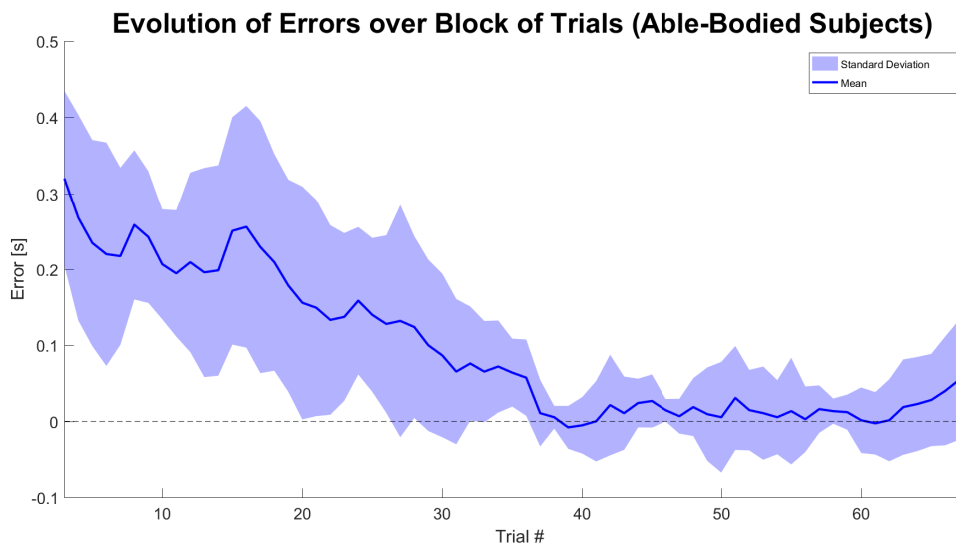


Figure 1.3.1: Evolution of error magnitude for able-bodied subjects over one block of 70 trials. The shaded region shows the standard deviation of error value of all subjects for each trial, the curve shows the mean error of all subjects for each trial with a moving average filter (size = 5).

In JND testing, the difference between JND after the 25th reversal to the n th reversal was compared and visualized (see Figure 1.3.1). Only marginal changes in mean and standard deviation ($0.24\% \pm 2.05\%$) are observed from reversal 22 onwards. Values for mean and standard deviation are converging from reversal 5 onwards. Between trial 15 and 22, some convergence is visible, although less prominent than between reversals 5 and 15.

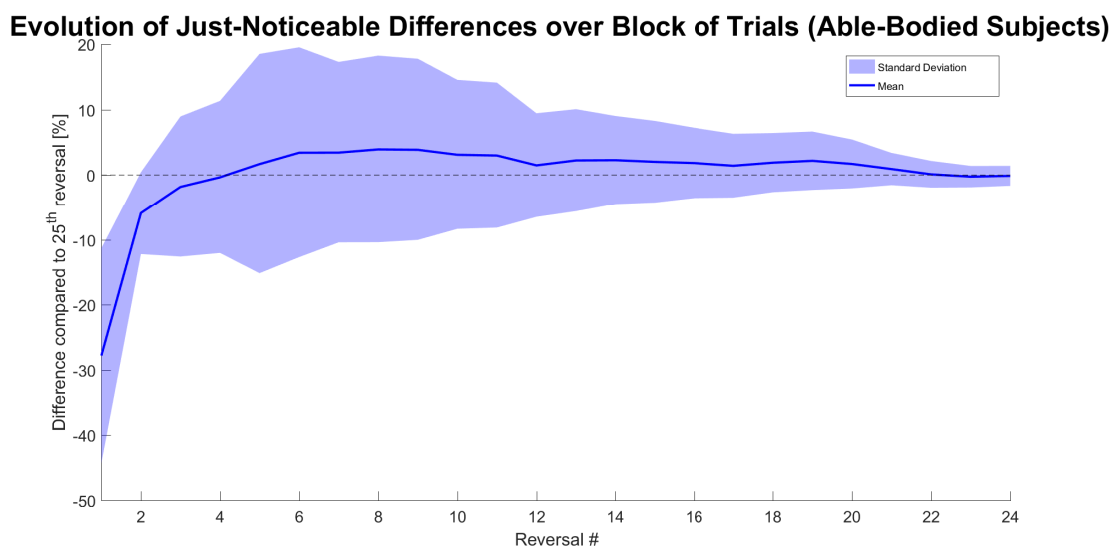


Figure 1.3.2: Evolution of JND for able-bodied subjects over one block with 25 reversals. Variations over reversals are calculated by subtracting JND after 25th reversal from JND after respective reversal.

1.3.1.2 Frame of Reference for Outcome Values

Adaptation rates are reported at 30, 40, 50, 60, and 70. As indicated by Figure 1.3.1, there is some discrepancy as to the number of trials AR should be analysed for. An evaluation of how AR values are impacted by the choice of analysis interval is visualized in Figure 1.3.3.

**Adaptation Rate with Cutoff at different Trial Numbers
(Able-Bodied Subjects)**

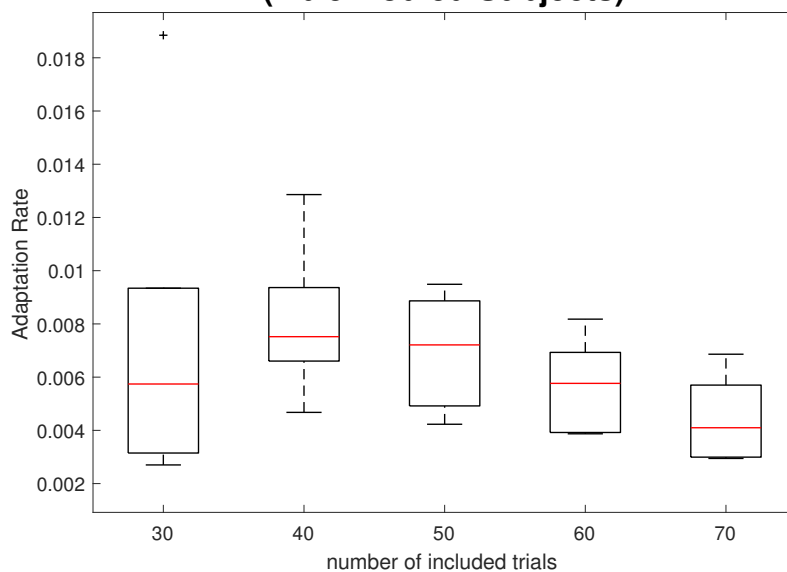


Figure 1.3.3: Adaptation rates for able-bodied subjects calculated with different cutoff points. Median values are $5.7 \cdot 10^{-3}$ for cutoff at 30, $7.5 \cdot 10^{-3}$ for cutoff at 40, $7.2 \cdot 10^{-3}$ for cutoff at 50, $5.8 \cdot 10^{-3}$ for cutoff at 60, and $4.1 \cdot 10^{-3}$ for cutoff at 70 trials. Boxplot midline represents the median, edges of each box show the 25th and 75th percentile. Outliers are noted by a ‘+’.

After the mark of trial 40, differences between subjects decrease, and individual results are increasingly difficult to recognize. The median AR is equal to $7.2 \cdot 10^{-3}$ at maximum (trials 1 to 40 included) and equal to $4.1 \cdot 10^{-3}$ at minimum (trials 1 to 70 included). It is notable that values were considerably lower than those observed in [22].

The just-noticeable differences showed high inter-subject variability, with results ranging from 22.96% to 78.96% after 20 reversals, and 24.38% to 75.52% after 25 reversals, respectively (see Figure 1.3.4. Only marginal changes are visible between results after 20 and 25 reversals.

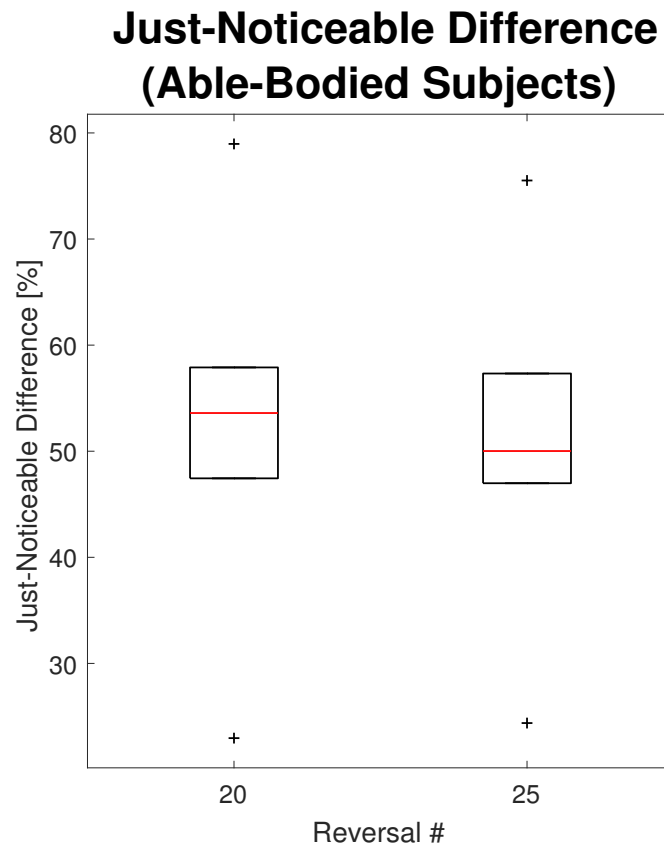


Figure 1.3.4: Just-noticeable differences for able-bodied subjects after 20 and 25 reversals. Median values are 53.6% after 20 reversals and 50.0% after 25 reversals. Boxplot midline represents the median, edges of each box show the 25th and 75th percentile. Outliers are noted by a ‘+’.

1.3.2 Experiment B

1.3.2.1 Stimulation Parameters

Stimulation parameters were determined according to the procedure described above. Minimum and maximum values for stimulation parameters can be found in Table 3. Locations of perception for the minimum, intermediate, and maximum parameters are visualized in Figures PD and PA. Intensities of used stimuli are shown in Table 4. Modulation of pulse amplitude only changed the intensity of perception (see Table 1.3.2b). Pulse width mainly altered the location and size of the field of perception, although a small increase in intensity was also observed (see Table 1.3.2a). Additional to this quantification of perceptions, the subject was asked to describe each percept with his own words. For increasing amplitude, the pulses were described as a “pinch” with increasing intensity. For different pulse widths, the perception was described as “diffuse” and “hard to point” for pulse widths of 400 μ s and 500 μ s, whereas pulses of 200 μ s duration were similar to a “pinch”. Further, the width modulated pulses were described as “electrical” and spreading like “rings on water” rather than “natural”.

Parameter	Label	Value
Electrode Surface Area	$A[\text{mm}^2]$	1.48
Duration of stimulating phase of a stimulus pulse	$D[\mu\text{s}]$	200-500
Duration of reversal phase of a stimulus pulse	$D_r[\mu\text{s}]$	2000-5000
Frequency	$F[\text{Hz}]$	25
Current of stimulating phase	$I[\mu\text{A}]$	390-500
Current of reversal phase	$I_r[\mu\text{A}]$	39-50
Number of pulses per train	N	25
Total time	$P[\text{hrs}]$	5
Effective stimulation time	$S[\text{hrs}]$	0.94
Inter-phase delay	$W[\mu\text{s}]$	50
Amplitude of stimulating and reversal phase ratio	c	10
Charge of stimulating phase per unit area	$QD[\text{nC}/\text{mm}^2]$	52.7-168.9
Percentage of effective stimulation time	$O[\%]$	18.75
Charge of stimulating phase	$Q[\text{nC}]$	78-250
Train rate	$R[\text{Hz}]$	0.1875
Train duration	$T[\text{s}]$	1
Weighted frequency of effective stimulation	$wF[\text{Hz}]$	4.69

Table 1.3.1: Stimulation Parameters.

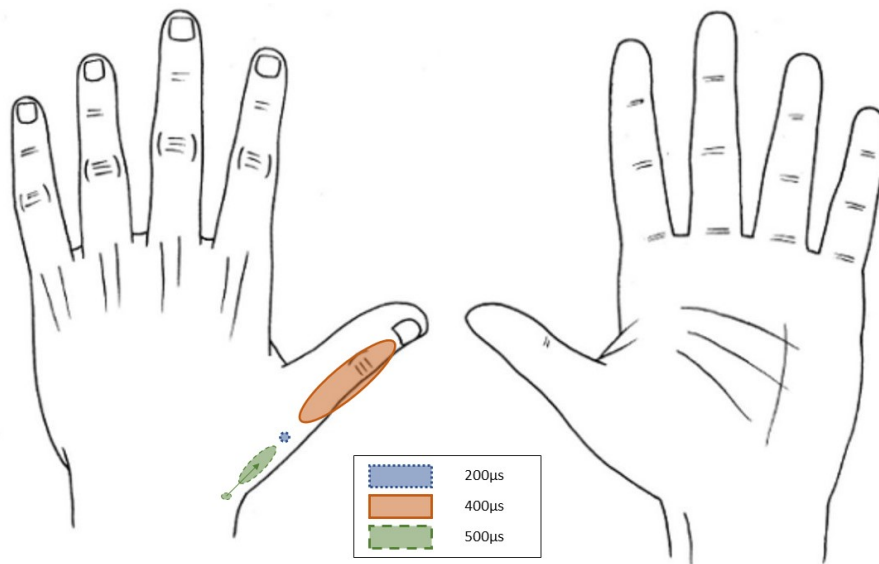


Figure 1.3.5: Location of sensation for different pulse widths (blue = 200 μs , red = 400 μs , green = 500 μs). $I = 400\mu\text{A}$; $F = 25\text{Hz}$; $N = 2$. The 200 μs pulses were perceived in a small, refined area. The 400 μs pulses were perceived in a larger area along the thumb. The 500 μs pulses were perceived first to a small area near the wrist and then moved up towards the thumb. The intensity of perception was identical for pulse pairs with 200 μs and 400 μs duration but increased for pulse pairs with 500 μs duration (see Table 1.3.2a).

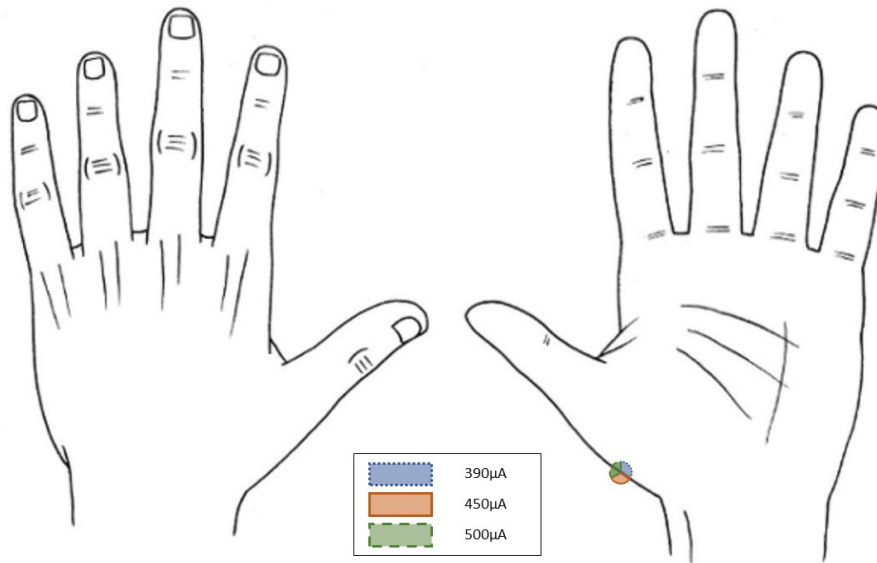


Figure 1.3.6: Location of sensation for different pulse amplitudes (blue = $390\mu\text{A}$, red = $450\mu\text{A}$, green = $500\mu\text{A}$). $W = 200\mu\text{s}$; $F = 25\text{Hz}$; $N = 2$. All pulse pairs of different amplitude were perceived in the same refined location, only intensity of the perception increased (see Table 1.3.2b).

D [μs]	Perceived intensity
200	3
400	3
500	4

(a) Intensity for each combination of parameters (width modulation).

I [μA]	Perceived intensity
390	3
450	4
500	5

(b) Intensity for each combination of parameters (amplitude modulation).

Table 1.3.2: Perceived intensities for different parameters.

1.3.2.2 Augmented feedback and different modulation paradigms

The adaptation rate and the just-noticeable difference was evaluated for each feedback modality. All results are displayed in the order of which the tests were conducted, therefore: VSA-SA-VSW-SW-V.

The evolution of errors was visualized and taken into consideration for adaptation rate analysis. All feedback conditions including visual feedback, therefore V, VSA, and VSW, show convergence to a temporary “steady state” at trial 20-30, whereas SA and SW do not show any convergence. It is noticeable that both feedback modalities, although no adaptation is visible, show low error values throughout the trial block. These errors are smaller than those observed for feedback conditions including visual feedback. Further, an increase in error magnitude towards the end of each block is observable (see Figure 1.3.7).

1. Assessment of Internal Model Strength based on augmented feedback

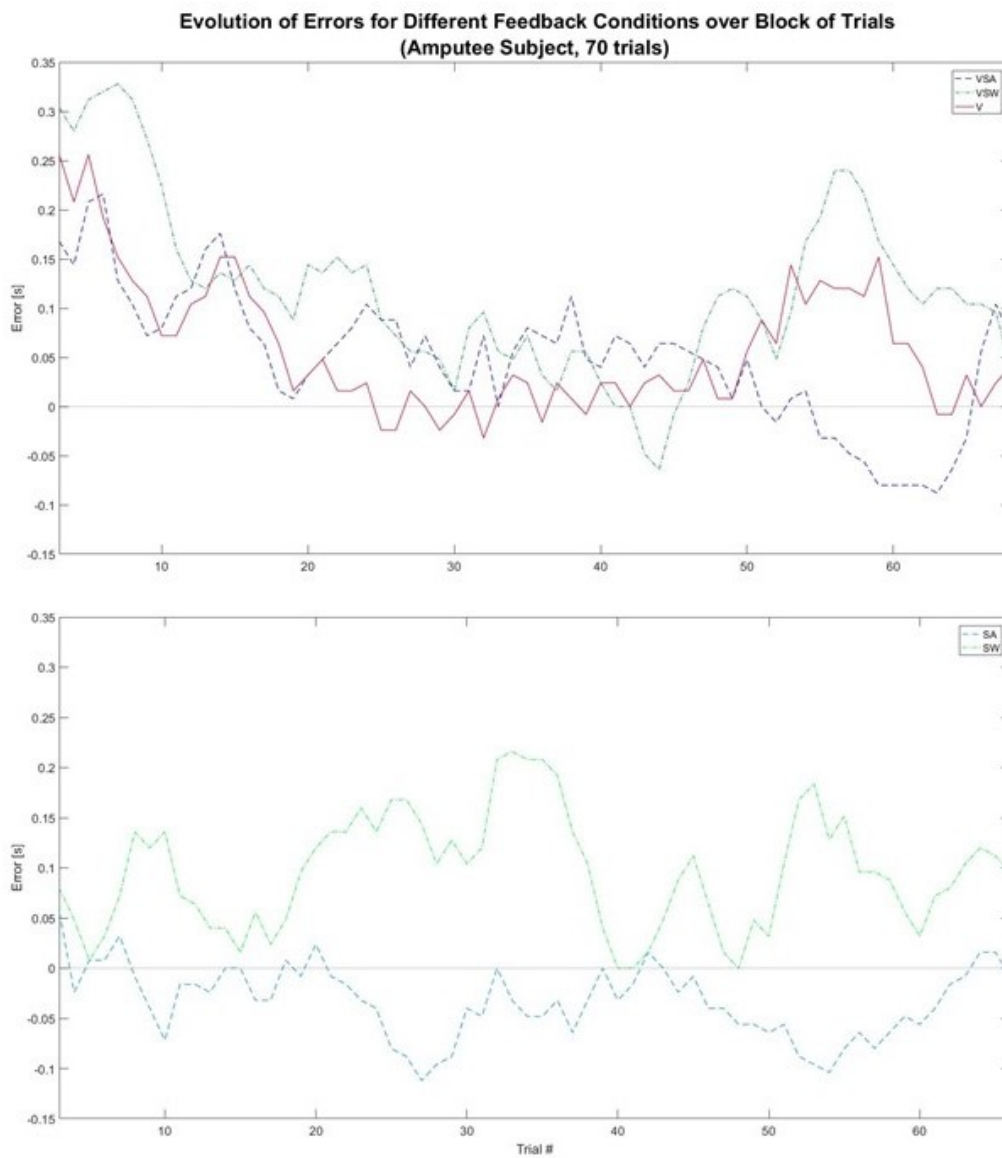


Figure 1.3.7: Evolution of error magnitude for different feedback conditions for amputee subject over one block of 70 trials. Errors are filtered with a moving average filter (size=5). The upper plot shows feedback conditions including visual feedback. The lower plot shows feedback condition excluding visual feedback.

**Adaptation Rate for Different Feedback Conditions
(Amputee Subject, 50 Trials)**

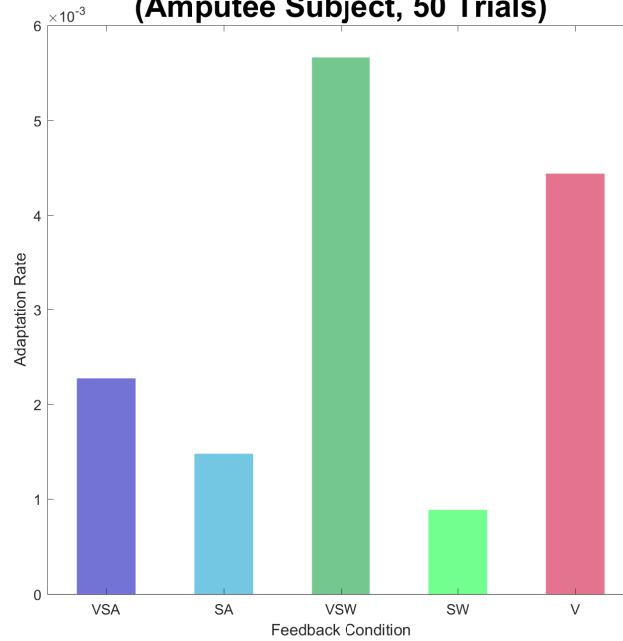


Figure 1.3.8: Conventional adaptation rate and absolute errors for different feedback conditions over 50 trials by amputee subject. Adaptation rates are $2.3 \cdot 10^{-3}$ for VSA, $1.5 \cdot 10^{-3}$ for SA, $5.7 \cdot 10^{-3}$ for VSW, $0.9 \cdot 10^{-3}$ for SW, and $4.4 \cdot 10^{-3}$ for V.

Due to observations in error evolution described above, the adaptation rate was calculated for trials 1 to 50. Feedback conditions including visual feedback show larger ARs than those without. Results for augmented feedback are somewhat discrepant; feedback condition VSW showed a higher AR than V, however, AR for VSA is much lower than the other two (see Figure 1.3.8).

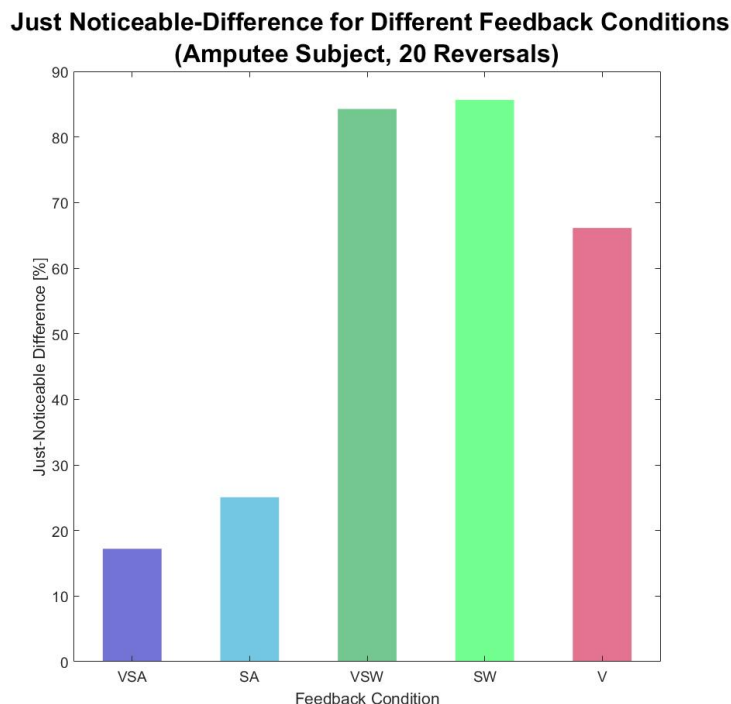


Figure 1.3.9: Just-noticeable difference after 20 reversals for different feedback conditions by amputee subject. Just-noticeable differences are 17.2% for VSA, 25.1% for SA, 84.3% for VSW, 85.7% for SW, and 66.1% for V.

Just-noticeable differences show a clear advantage for feedback conditions including sensory feedback with amplitude modulation, VSA and SA. Here the JNDs were 17.2% and 25.1%, respectively. Results for conditions with sensory feedback with width modulation differ to a great extent, with VSW and SW showing a much larger JNDs than VSA and SA. A 67.1% increase was observed from VSA to VSW, and a 60.6% increase from SA to SW. For visual feedback, V, the JND is smaller (66.1%) than for feedback conditions including width modulated sensory feedback, however, it seems to be inferior to feedback conditions including amplitude modulated sensory feedback (see Figure 1.3.9).

1.3.2.3 Comparison of Outcome Parameters Experiment A versus Experiment B

In AR testing, the amputee subject generally scored lower than able-bodied subjects, with results ranging from $0.9 \cdot 10^{-3}$ to $5.7 \cdot 10^{-3}$ compared to $4.2 \cdot 10^{-3}$ to $9.5 \cdot 10^{-3}$. However, considering the evolution of errors over each trial block (see Figures 1.3.1 and 1.3.7) a smaller magnitude of the initial error can be observed for the amputee subject. This difference between able-bodied subjects and amputee subject could not be observed for JND testing; here ranges for able-bodied and amputee were 23-79% and 17-86%, respectively. However, JND showed much larger inter-subject variability than AR.

1.4 Discussion

The trial-by-trial adaptation and the just-noticeable difference were evaluated for six able-bodied subjects for one feedback condition (Experiment A) and one amputee subject for five feedback conditions (Experiment B).

1.4.1 Task Parameters

Both, Experiment A and Experiment B showed that an adaptation of the task duration to EMG control is necessary. In the AR testing, 70 trials proved to be too many. A “steady state” was reached by both groups between trial 20 and 40. This “steady state” was then followed by an increase in error values after trial 50 for the amputee subject and 60 for the able-bodied group. This increase in error could be an indicator of muscle fatigue, decrease in concentration, or a combination of both.

In JND testing, for the amputee subject, the number of reversals was reduced from 25 to 20 in order to reduce the time required for each block. The results from able-bodied subjects showed this reduction to be viable, as results only varied marginally.

In tests for amputee or rehabilitation patients keeping the balance between the most exact measure and as little fatigue as possible is of high importance, as this subject group is extremely susceptible to fatigue and, thus, reduced levels of concentration. Amputees using a myoelectric prosthesis on an everyday basis, however, are expected to learn a new myoelectric control pattern faster than an untrained able-bodied subject, therefore using a similar cutoff in adaptation rate calculation seems viable. It must be kept in mind, that inter-subject variability must be accounted for, therefore a cutoff of 50 rather than 70 trials is advised for future experiments.

1.4.2 EMG Control

One of the downfalls of EMG control is a high variability in the EMG signal. This variability is even more pronounced in a task as short as one second. Further, a limitation of this study was the unusually low sampling frequency used for EMG (250Hz). As the relevant frequency range for EMG is commonly defined as 20-500Hz [29], much valuable information was lost. The sampling frequency was the highest achievable frequency with the current setup, as concluded after initial benchmark testing (see also [30]). Another factor is the rigid controller. Using a lower level of contraction for maximum speed should increase controllability, as signal variability in EMG is influenced by the level of contraction. Further, muscle fatigue is minimal for percentages below 85% of the MVC [31].

An additional technique to lower variability and uncertainty in the controller is the introduction of larger time windows for control enabled by the overlap of acquisition windows.

1.4.3 Latency

A factor that must be considered, is the latency between EMG activity and controller reaction, as well as latency between visual and sensory feedback. In similar publications, the latency between EMG activity and controller was around 60ms [7]. In this case, the latency in communication between Matlab and the ALC was equal to 6.7 ± 0.69 ms [30], therefore in an acceptable range. Latency between visual and sensory feedback that has been found to influence sensory integration (e.g. [9]) with this specific device was tested in another work [30]. A delay of 100ms of the neurostimulation was found to be perceived as simultaneous by one subject, however, these results were not considered here.

1.4.4 Sensory feedback by electrical stimulation of peripheral nerves

Although investigated in recent studies [15–19, 32, 33] decoding neural excitation patterns remains a challenge. In this study, pulses of varying duration and amplitude were examined. In accordance with previous research (e.g. [17]), modulation of pulse amplitude only changed the intensity of perception (see Table 1.3.2b). Width modulation had an effect on both perceived intensity and location of the perceived sensation. Closer examination of these patterns was not subject of this study.

1.4.5 Feedback Modalities

Results for different feedback conditions in the amputee subjects showed some discrepancy. The hypothesis that augmented feedback enable better scores, and therefore a higher AR and a lower JND, could neither be clearly confirmed nor rejected.

The JND testing showed exceptionally low JNDs for those feedback conditions including sensory feedback by amplitude modulation, however, conditions including width modulated sensory feedback were inferior to the visual-only condition. Therefore, augmented feedback proved to be beneficial in one case (VSA), but distracting in the other (VSW). Further, singular, sensory feedback resulted in better scores in one case (SA) even than visual feedback but turned out to be distracting for the other (SW). Therefore, the influence of the mode of sensory feedback seems to be much larger than that of augmented versus limited feedback. The subject reached a lower JND, therefore a better result, in both augmented compared to singular feedback conditions. However, this effect was observed to be marginal.

Results for adaptation rate are more difficult to interpret. There is a clear advantage of feedback conditions including visual feedback over those that are solely sensory. However, one augmented feedback condition (VSW) scored higher than the visual (V) condition, whereas the other (VSA) scored lower. A potential reason for these results is the way the adaptation rate is commonly calculated. It does not account for variation learning curves, where the subject reaches a "steady state" (therefore, errors similar over several trials, where errors = 0). Further, the initial magnitude of errors is not considered. In this case, the magnitude of initial errors in VSW

feedback condition is larger than that in VSA and V feedback conditions, therefore analysis is somewhat biased towards this condition.

For non-visual feedback conditions (SA, SW) low AR scores were observed. However, especially in the SA condition low error magnitudes can be observed early on in the block. Therefore, the whole AR block could be considered as "steady state". In order to improve these flaws in analysis, an improved experiment layout will be helpful, but a requirement for more advanced methods in the analysis of learning rates is apparent.

Considering both conducted tests equally, a meaningful evaluation of singular versus augmented feedback and of different pulse modulation techniques is impossible; in the AR testing, width modulation seemed to be advantageous, whereas in JND testing amplitude modulation resulted in superior scores. Visual feedback was in AR testing located between both types of augmented feedback. In JND testing, visual feedback was inferior to both feedback conditions containing width modulated sensory feedback.

Due to the bias introduced to AR evaluation, JND testing should be highlighted. Here, feedback conditions containing amplitude modulated sensory feedback are clearly superior to those containing width modulated feedback. Further, augmented show better scores than singular feedback conditions.

A solution to biased AR testing could be evaluating the number of trials required to reach "steady state" combined with the magnitude of initial and "steady" error. This way, a subject's experience or initial abilities, hence low initial error magnitude, could be taken into account.

Another factor that must be taken into account, is the order of testing, as it introduces a clear bias towards those feedback conditions tested early on. This is due to both fatigue during testing as well as increased boredom. It is highly likely that the subject's performance was impaired by these two factors.

1.4.6 Limitations

Limitations of a study with a low number of subjects are clear: results are highly individual and linked to experience with EMG control. Naturally, an amputee using an EMG controlled prosthetic for years will achieve lower errors than completely untrained subjects.

A permanent bias in applying proportional control is the individually varying ranges. A subject with stronger muscles, will be able to produce a larger range and therefore has better control compared to a "weaker" subject.

1.5 Conclusion

The experiment design was flawed and a pilot study with able-bodied subjects to identify these flaws was conducted only after they became apparent. For future studies, this procedure must be improved.

The main issues in the experiment layout were a too low EMG sampling rate that neglected valuable frequencies, extensive experiment duration that lead to fatigue and boredom in subjects, and a limited number of subjects, that made meaningful data analysis difficult.

Nonetheless, there is some indication, especially in JND test results, that augmented feedback, could be advantageous in internal model formation and, consequently, in prosthesis functionality. This applies especially to sensory feedback with amplitude modulated pulses. These indicators could be amplified by an improved experiment protocol, that must be confirmed through thorough testing with a large group of able-bodied subjects.

1.6 Outlook

Major improvements for future experiments include:

1. a higher sampling rate of at least 1kHz to enable analysis of the complete EMG frequency range;
2. lower trial numbers for:
 - (a) adaptation rate test (suggestion 50 trials);
 - (b) just-noticeable difference test (suggestion 20 reversals);
3. a maximum of one feedback condition per day to prevent bias induced by fatigue and boredom; and
4. adaptation of controller parameters to rest and a value $< 85\%$ of the MVC.

With the initial aims of the study in mind, only an ambiguous conclusion can be drawn. The task developed by Blustein and Sensinger was expanded to EMG control and NS feedback, although control parameters remain to be improved in the next iteration of this work. The value of augmented feedback proved to be highly related to the mode of stimulation applied. In a study limited to one individual, it was clear that feedback, both singular and augmented, by amplitude modulation improved the level of performance to a large extent. Sensory feedback by width modulated pulses, however, proved to be distracting rather than helpful. This outcome can, to some degree, be connected to the order of feedback conditions tested.

References

- [1] I. Saunders and S. Vijayakumar, “The role of feed-forward and feedback processes for closed-loop prosthesis control”, *Journal of NeuroEngineering and Rehabilitation*, vol. 8, no. 1, pp. 1–12, 2011.

- [2] M. A. Schiefer, D. W. Tan, S. M. Sidek, and D. J. Tyler, “Sensory feedback by peripheral nerve stimulation improves task performance in individuals with upper limb loss using a myoelectric prosthesis”, *Journal of Neural Engineering*, vol. 13, no. 1, p. 016001, 2016.
- [3] D. M. Wolpert, J. Diedrichsen, and J. R. Flanagan, “Principles of sensorimotor learning”, *Nature Reviews Neuroscience*, vol. 12, no. 12, 2011.
- [4] B. A. Francis and W. M. Wonham, “The Internal Model Principle of Control Theory The Internal Model Principle of Control Theory *”, *Automatica*, vol. 12, no. 5, pp. 457–465, 1976.
- [5] M. Kawato, K. Furukawa, and R. Suzuki, “A Hierarchical Neural-Network Model for Control and Learning of Voluntary Movement”, *Biological Cybernetics*, vol. 57, pp. 169–185, 1987.
- [6] M. Kawato, “Internal models for motor control and trajectory planning”, *Curr.Opin.Neurobiol.*, vol. 9, no. 6, pp. 718–727, 1999.
- [7] S. Dosen, M. Markovic, N. Wille, M. Henkel, M. Koppe, A. Ninu, C. Frömmel, and D. Farina, “Building an internal model of a myoelectric prosthesis via closed-loop control for consistent and routine grasping”, *Experimental Brain Research*, vol. 233, no. 6, pp. 1855–1865, 2015.
- [8] A. W. Shehata, E. J. Scheme, and J. W. Sensinger, “Myoelectric Prosthesis Control: Improving Internal Model Strength and Performance using Augmented Feedback”, 2018.
- [9] D. W. Franklin and D. M. Wolpert, “Computational mechanisms of sensorimotor control”, *Neuron*, vol. 72, no. 3, pp. 425–442, 2011.
- [10] T. R. Clites, M. J. Carty, J. B. Ullauri, M. E. Carney, L. M. Mooney, J.-F. Duval, S. S. Srinivasan, and H. M. Herr, “Proprioception from a neurally controlled lower-extremity prosthesis”, *Science translational medicine*, vol. 10, no. 443, eaap8373, 2018.
- [11] S. M. Radhakrishnan, S. N. Baker, and A. Jackson, “Learning a Novel Myoelectric-Controlled Interface Task”, *Journal of Neurophysiology*, vol. 100, no. 4, pp. 2397–2408, 2008.
- [12] K. P. Körding and D. M. Wolpert, “Bayesian integration in sensorimotor learning”, *Nature*, vol. 427, no. 6971, pp. 244–247, 2004.
- [13] A. Ninu, S. Dosen, S. Muceli, F. Rattay, H. Dietl, and D. Farina, “Closed-Loop Control of Grasping With a Myoelectric Hand Prosthesis: Which Are the Relevant Feedback Variables for Force Control?”, *IEEE Transactions on Neural Systems and Rehabilitation Engineering*, vol. 22, no. 5, pp. 1041–1052, 2014.
- [14] D. M. Wolpert and M. Kawato, “Multiple paired forward and inverse models for motor control”, *Neural Networks*, vol. 11, no. 7-8, pp. 1317–1329, 1998.
- [15] R. Ackerley, H. Backlund Wasling, M. Ortiz-Catalan, R. Brånemark, and J. Wessberg, “Case Studies in Neuroscience: sensations elicited and discrimination ability from nerve cuff stimulation in an amputee over time”, *Journal of Neurophysiology*, 2018.
- [16] D. W. Tan, M. A. Schiefer, M. W. Keith, J. R. Anderson, J. Tyler, and D. J. Tyler, “A neural interface provides long-term stable natural touch perception”, *Science Translational Medicine*, vol. 6, no. 257, 257ra138, 2014.

- [17] E. L. Graczyk, M. A. Schiefer, H. P. Saal, B. P. Delhaye, S. J. Bensmaia, and D. J. Tyler, “The neural basis of perceived intensity in natural and artificial touch”, *Science Translational Medicine*, vol. 8, no. 362, 362ra142, 2016.
- [18] C. M. Oddo, S. Raspopovic, F. Artoni, A. Mazzoni, G. Spigler, F. M. Petrini, F. Giambattistelli, F. Vecchio, F. Miraglia, L. Zollo, G. Di Pino, D. Camboni, M. C. Carrozza, E. Guglielmelli, P. M. Rossini, U. Faraguna, and S. Micera, “Intraneural stimulation elicits discrimination of textural features by artificial fingertip in intact and amputee humans”, *eLife*, vol. 5, pp. 1–27, 2016.
- [19] S. Raspopovic, M. Capogrosso, F. M. Petrini, M. Bonizzato, J. Rigosa, G. Di Pino, J. Carpaneto, M. Controzzi, T. Boretius, E. Fernandez, G. Granata, C. M. Oddo, L. Citi, A. L. Ciancio, C. Cipriani, M. C. Carrozza, W. Jensen, E. Guglielmelli, T. Stieglitz, P. M. Rossini, and S. Micera, “Restoring Natural Sensory Feedback in Real-Time Bidirectional Hand Prostheses”, *Science Translational Medicine*, vol. 6, no. 222, 222ra19, 2014.
- [20] A. B. Anani, K. Ikeda, and L. M. Körner, “Human ability to discriminate various parameters in afferent electrical nerve stimulation with particular reference to prostheses sensory feedback”, *Medical & Biological Engineering & Computing*, vol. 15, no. 4, pp. 363–373, 1977.
- [21] F. W. Clippinger, R. Avery, and B. R. Titus, “A sensory feedback system for an upper-limb amputation prosthesis”, *Bulletin of prosthetics research*, pp. 247–258, 1974.
- [22] D. H. Blustein and J. W. Sensinger, “Validation of a constrained-time movement task for use in rehabilitation outcome measures *”, *2017 International Conference on Rehabilitation Robotics (ICORR), London, 2017*, pp. 1183–1188, 2017.
- [23] E. Mastinu, P. Doguet, Y. Botquin, B. Håkansson, and M. Ortiz-Catalan, “Embedded System for Prosthetic Control Using Implanted Neuromuscular Interfaces Accessed Via an Osseointegrated Implant”, *IEEE Transactions on Biomedical Circuits and Systems*, vol. 11, no. 4, pp. 867–877, 2017.
- [24] M. Ortiz-Catalan, B. Håkansson, and R. Brånemark, “An osseointegrated human-machine gateway for long-term sensory feedback and motor control of artificial limbs”, *Science Translational Medicine*, vol. 6, no. 257, 257re6, 2014.
- [25] C. Günter, J. Delbeke, and M. Ortiz-catalan, “Safety of long-term electrical peripheral nerve stimulation: review of the state of the art”, vol. 8, pp. 1–16, 2019.
- [27] R. E. Johnson, K. P. Körding, L. J. Hargrove, and J. W. Sensinger, “Adaptation to random and systematic errors: Comparison of amputee and non-amputee control interfaces with varying levels of process noise”, *PLoS ONE*, vol. 12, no. 3, pp. 1–19, 2017.
- [28] L. Faes, G. Nollo, F. Ravelli, L. Ricci, M. Vescovi, M. Turatto, F. Pavani, and R. Antolini, “Small-sample characterization of stochastic approximation staircases in forced-choice adaptive threshold estimation”, *Perception & Psychophysics*, vol. 69, no. 2, pp. 254–262, 2007.
- [29] C. J. DeLuca, “The use of surface electromyography in biomechanics”, *Clinical Biomechanics*, vol. 13, pp. 135–163, 1997. arXiv: [arXiv:1011.1669v3](https://arxiv.org/abs/1011.1669v3).

- [31] E. A. Müller, “Physiological methods of increasing human physical work capacity.”, *Ergonomics*, vol. 8, no. 4, pp. 409–424, 1965.
- [32] M. Ortiz-Catalan, E. Mastinu, R. Brånemark, and B. Håkansson, “Direct Neural Sensory Feedback and Control via Osseointegration”, *XVI World Congress of the International Society for Prosthetics and Orthotics (ISPO)*, Cape Town, South Africa, May 8–11, 2017.
- [33] G. A. Clark, S. Wendelken, D. M. Page, T. Davis, H. A. C. Wark, R. A. Normann, D. J. Warren, and D. T. Hutchinson, “Using multiple high-count electrode arrays in human median and ulnar nerves to restore sensorimotor function after previous transradial amputation of the hand”, *36th Annual International Conference Proceedings of IEEE Engineering in Medicine and Biology Society (EMBC)*, pp. 1977–1980, 2014. eprint: NIHMS150003.

2

Safety of long-term electrical peripheral nerve stimulation

REVIEW

Open Access



Safety of long-term electrical peripheral nerve stimulation: review of the state of the art

Clara Günter¹, Jean Delbeke² and Max Ortiz-Catalan^{1,3*} 

Abstract

Background: Electrical stimulation of peripheral nerves is used in a variety of applications such as restoring motor function in paralyzed limbs, and more recently, as means to provide intuitive sensory feedback in limb prostheses. However, literature on the safety requirements for stimulation is scarce, particularly for chronic applications. Some aspects of nerve interfacing such as the effect of stimulation parameters on electrochemical processes and charge limitations have been reviewed, but often only for applications in the central nervous system. This review focuses on the safety of electrical stimulation of peripheral nerve in humans.

Methods: We analyzed early animal studies evaluating damage thresholds, as well as more recent investigations in humans. Safety requirements were divided into two main categories: passive and active safety. We made the distinction between short-term (< 30 days) and chronic (> 30 days) applications, as well as between electrode preservation (biostability) and body tissue healthy survival (harmlessness). In addition, transferability of experimental results between different tissues and species was considered.

Results: At present, extraneural electrodes have shown superior long-term stability in comparison to intraneural electrodes. Safety limitations on pulse amplitude (and consequently, charge injection) are dependent on geometrical factors such as electrode placement, size, and proximity to the stimulated fiber. In contrast, other parameters such as stimulation frequency and percentage of effective stimulation time are more generally applicable. Currently, chronic stimulation at frequencies below 30 Hz and percentages of effective stimulation time below 50% is considered safe, but more precise data drawn from large databases are necessary. Unfortunately, stimulation protocols are not systematically documented in the literature, which limits the feasibility of meta-analysis and impedes the generalization of conclusions. We therefore propose a standardized list of parameters necessary to define electrical stimulation and allow future studies to contribute to meta-analyses.

Conclusion: The safety of chronic continuous peripheral nerve stimulation at frequencies higher than 30 Hz has yet to be documented. Precise parameter values leading to stimulation-induced depression of neuronal excitability (SIDNE) and neuronal damage, as well as the transition between the two, are still lacking. At present, neural damage mechanisms through electrical stimulation remain obscure.

Keywords: Electrical stimulation, Safety, Peripheral nervous system, Nerve stimulation, Implants

* Correspondence: maxo@chalmers.se

¹Biomechanics and Neurorehabilitation Laboratory, Department of Electrical Engineering, Chalmers University of Technology, 41296 Gothenburg, Sweden

³Integrum AB, Krokslätts Fabriker 50, 43137 Mölndal, Sweden

Full list of author information is available at the end of the article



© The Author(s). 2019 **Open Access** This article is distributed under the terms of the Creative Commons Attribution 4.0 International License (<http://creativecommons.org/licenses/by/4.0/>), which permits unrestricted use, distribution, and reproduction in any medium, provided you give appropriate credit to the original author(s) and the source, provide a link to the Creative Commons license, and indicate if changes were made. The Creative Commons Public Domain Dedication waiver (<http://creativecommons.org/publicdomain/zero/1.0/>) applies to the data made available in this article, unless otherwise stated.

Introduction

Despite numerous applications and the reported benefits of peripheral nerve stimulation, descriptions of specific safety requirements remain scarce. Agnew and McCreery, who authored a number of papers on safety aspects of electrical stimulation of peripheral nerves in cats, reviewed and summarized their findings almost three decades ago [1]. The literature on safe, long-term, and continued stimulation of peripheral nerves has grown marginally since then. More recent reviews have addressed general safety aspects of neural stimulation with particular focus on electrochemical processes [2, 3], mainly with regards to stimulation of the central nervous system [4].

Various applications require direct peripheral nerve stimulation. Prostheses involving motor nerve stimulation include respiratory ventilation [5] and correction of foot drop [6]. More recently, promising results have been obtained stimulating afferent fibers for prosthetic sensory feedback in acute [7–16] and chronic experiments [17–22].

Safety aspects of electrical stimulation are particularly crucial in chronic applications. Safety considerations range from the assessment of biostability (including passive electrode preservation and maintained functionality despite the implanted tissue reaction) and harmlessness through the identification of acceptable limits for various electrical stimulation parameters. Animal experiments raise questions about inter-species transferability. Even within the same species, results cannot always be extrapolated from one tissue to the other (central versus peripheral nervous system). Furthermore, within the peripheral nervous system, different nerve fibers conduct action potentials at different speeds [23], and variable frequency and duration [24], which can affect their tolerance to electrical stimulation regimes. On the basis of an overview of recent literature, we aim at inferring essential safety rules governing peripheral nerve stimulation in humans.

Passive safety

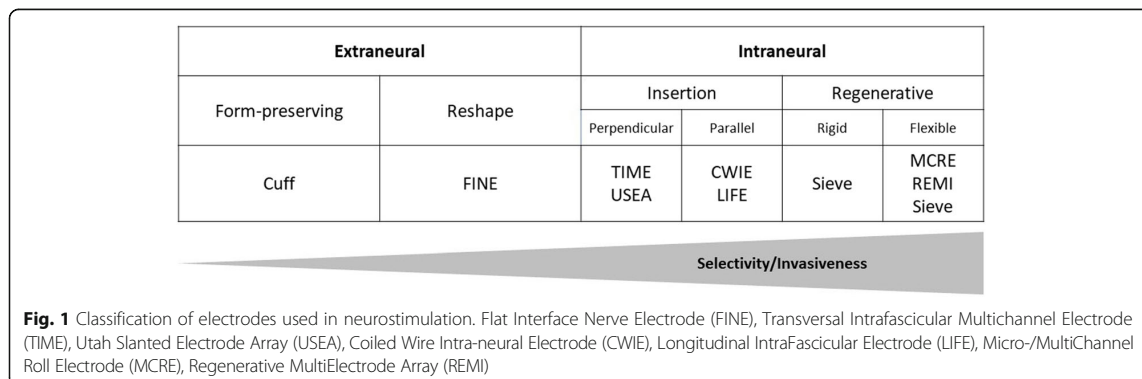
Various types of highly sophisticated and specialized electrodes have been developed for interfacing with the nervous system. Here, we classify electrodes in terms of size, material, and electrochemical properties, as well as local safety aspects in terms of biostability and harmlessness. Issues not specific to electrodes such as toxicity of leaching chemicals, infection risks, and surgery-linked side effects were not incorporated in this review.

Structural classification

Interaction of electrodes can be expected to be different according to the tissue component in contact (epineurium, perineurium, and endoneurium). The formation of a fibrous encapsulation can modify this situation and result in functional changes over time. As suggested in a review by Kim and Romero-Ortega [25], electrodes used in peripheral nerve stimulation can be broadly classified as extra- or intra-neural, before being further divided in subcategories (Fig. 1).

Extraneural electrodes are applied outside the epineurium. They may allow the nerve to remain essentially in its original shape, as with cuff electrodes [26], or have selectivity-improving reshaping characteristics, as with the flat interface nerve electrodes (FINE) [27]. The more invasive intraneural electrodes penetrate the epineurium and can be further sub-divided into insertable or regenerative electrodes. Insertable electrodes may be implanted perpendicular or parallel to the nerve axis [28–30]. A further division into extra- and intra-fascicular electrodes is possible as their resting location would have a non-negligible effect on electrical stimulation, albeit fibrous tissue encapsulation of the electrode over time can make such distinction challenging. Regenerative electrode implantation includes an initial neural fiber transection followed by regeneration through regrowth. Rigid or flexible substrate designs have been proposed for this purpose [31–35].

The choice of electrode involves a trade-off between selectivity and invasiveness. Intraneural electrodes are



expected to be more advantageous when considering selectivity due to the short distance to target, whereas extraneural electrodes are less invasive but also less selective.

Data collected by Navarro et al. point to the fact that currently in clinical practice, implanted electrodes are generally extraneural [36]. Presently, with regards to long-term human implantations, extraneural electrodes still emerge as the most favorable choice for clinical applications [26, 37].

Electrical classification

In electrical terms, an electrode can roughly be described as a capacitor in parallel with a resistor. These model components vary for different contact interfaces. Electrodes can be classified as either ideally polarizable or ideally non-polarizable. An ideally polarizable electrode behaves predominantly as a capacitor and has a large resistive component, whereas the resistive component of 'ideally non-polarizable electrodes' is small enough for the capacitive component to be ignored. Correspondingly, the charge transfer at the electrode-electrolyte-interface is characterized as being capacitive (non-faradaic) or faradaic. A faradaic charge transfer involving ionic exchanges with the electrolyte through oxidation or reduction reactions is non-reversible unless the electrode is built in such a way that the reactions can continue indefinitely. A commonly used electrode of this type is the silver/silver-chloride electrode. Unfortunately, it cannot be implanted due to toxicity.

The capacitive charge transfer characterizing rapidly polarizable electrodes refers to a redistribution of local charges without electrochemical exchange. Within a very limited range, these capacitive processes are reversible. Some metals, such as platinum, exhibit a property named pseudocapacitance whereby, although a faradaic reaction occurs and electrons are effectively being transferred, the resulting products remain bound to the electrode surface and thus available to undo the chemical reactions. Hence, these reactions are also reversible.

Irreversible reactions must be avoided as their product accumulation will end up being harmful to the local tissues and/or to the electrode efficiency. This is of course a major issue for chronically implanted electrodes. The importance of using capacitive or pseudocapacitive processes to ensure reversibility of reactions was emphasized by Brummer and Turner in 1977 [38]. A more detailed description of electrochemical processes and electrical circuit models can be found in recent reviews [2, 4]. Methods such as cyclic voltammetry, impedance spectroscopy, and voltage transients [3] allow to characterize the electrochemical behavior of electrodes.

Biostability and harmlessness

The word 'biocompatibility' is often used ambiguously in the context of electrodes, referring to completely different issues. One meaning of the expression, which we shall refer to as 'harmlessness', describes how well the living organism tolerates and survives the implant without triggering unacceptable reactions or changes. We suggest limiting the concept of 'biostability' to designate the device resistance to the biologic medium and its ability to remain chronically functional after implantation. 'Biocompatibility' sums these aspects together and therefore is a requirement for any implantable device.

Harmlessness and biostability should be considered separately. Both these characteristics must be evaluated in active implanted devices as well as in the passive mode when the implant is idle (see Table 1). For example, corrosion is certainly activated by stimulation but can also be present at rest. Not only can this impair electrode function, but it also raises concerns about harmlessness; electrochemical by-products of corrosion can be toxic or trigger an exaggerated local inflammatory reaction. These distinctions are necessary to ensure that all potentially harmful aspects are addressed. Combining observations to conclude in terms of 'acceptable' or 'not acceptable' is not contributive to progress about these matters. Finally, one should not only consider the implanted electrode and the electrical stimulation, but also what can be called harmlessness of the therapy, looking at the effects of the therapy itself. The induction of damaging physiologic overload is an example of such a situation.

In chronic neural stimulation of various peripheral nerves in humans, extraneural electrodes have proven biostable in the peroneal nerve for at least 12 years [6] in passive and active testing. Similar compatibility was shown for up to 18 years stimulating the phrenic nerve [5]; up to 8 years stimulating the median, radial, sciatic, and ulnar nerves [39]; and up to 11 years stimulating motor and sensory nerves in a feedback controlled application [26]. Similarly, our research group has employed self-sizing spiral cuff electrodes to provide sensory feedback in prosthetic hands used outside the laboratory in daily-life activities [22] with no signs of neural damage or electrode deterioration after 18 months of uninterrupted use.

Table 1 Biocompatibility, biostability, and harmlessness

Biocompatibility	
Biostability	Harmlessness
The electrodes and their functionality	The damage to the organism
Passive	Idle conditions (no stimulation)
Active	Working conditions (stimulation)

Most often, electrodes implanted on peripheral nerves are made of Platinum-Iridium and Silicone. The passive biostability of the materials used to construct the electrode and leads are often determined from the documented use of the same products in other applications. Numerous studies have confirmed passive biostability of various electrode types. Similarly, local tissue reaction or tissue health after implantation has been mostly well-investigated. In terms of biological response to the electrode, Merrill et al. has developed a classification of tissue reactions to different materials [2]. Various biological responses to implanted materials were also discussed in depth by Anderson [40].

However, during surgery, peripheral nerves are sensitive to stretching [41], blood toxicity, and drying out [42]. They must therefore be handled most delicately during implantation. Initial issues with implantable extraneural electrodes often result from mechanical constriction and injury to the nerve during the surgical implantation process [43, 44]. Mechanical damage can also occur later. Electrode design evolved toward easy-to-apply constructions such as the Huntington helical electrode (used in e.g. [45]). Additionally, newer and more flexible spiral cuff electrodes [46, 47] leave room for nerve swelling immediately after implantation while still maintaining a snug fit for good electrical contact, and for preventing movement-induced injury [26]. Cylindrical cuff electrodes with elastic flaps have also been suggested as suitable in this regard by Loeb and Peck [48]. In addition to surgical challenges posed by electrode application, specific mechanical stress factors must be considered [49].

Intramuscular and epimysial electrodes seem to induce tissue responses similar to those of extraneural electrodes, including tissue encapsulation [50, 51]. Grill and Mortimer conducted research on tissue response to chronic implantation of extraneural electrodes [52] and on the input-output properties in terms of specific electrode current and the generated torque as a method to characterize selectivity [51]. After chronic implantation of spiral cuff electrodes around the cat sciatic nerve, as a foreign body reaction, they found connective tissue encapsulating the electrode in all cases. The neural tissue appeared healthy proximal to the cuffs, but showed moderate morphological changes at cuff level and somewhat more pronounced distal to the cuff in some cases [52]. With respect to input-output properties, Grill and Mortimer showed that the stimulus current amplitude required to generate a specific torque varies immediately after implantation, but becomes chronically stable after a period of 8 weeks. They assumed that this evolution mainly reflects the formation of fibrous tissue [51]. It was, however, not possible to find a direct correlation between the functional and

morphological changes observed. This was attributed to a low sensitivity of the measurement parameters, as well as several additional factors influencing the outcome, such as muscular hypertrophy compensating for loss of some motor units [52].

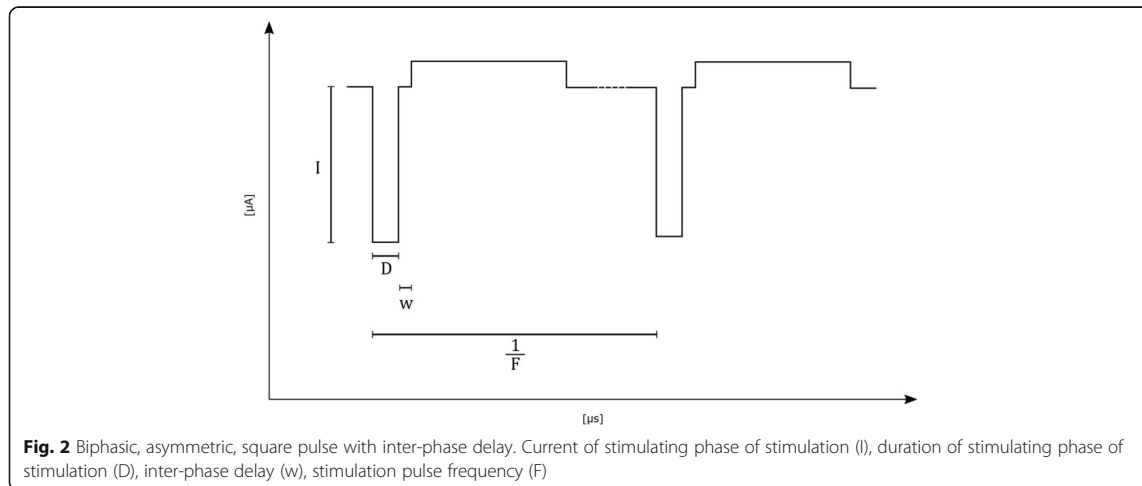
Girsch et al. and Larsen et al. showed that neural damage induced by the implantation and presence of an extraneural electrode is reversible [53, 54]. Girsch et al. assessed nerve lesions in the rat sciatic nerve 10 days, 3 weeks, and 3 months after cuff electrode implantation, and noted a gradual recovery from 4.74 to 0.57% of altered fascicular area. Larsen et al. evaluated axonal loss in the rabbit tibial nerve 2 weeks and 16 months after implantation of cuff electrodes, and demonstrated full regeneration after an initial loss of 27% of myelinated axons.

Concerning intraneural electrodes, Christensen et al. investigated the response to a Utah Slant Electrode Array (USEA) in the cat sciatic nerve and found strong tissue reactions, such as persistent active inflammation, even 22 to 26 weeks after implantation [55]. Lago et al. assessed the harmlessness of different longitudinal intrafascicular electrodes (LIFE), namely thin-film (tf-LIFE) and platinum (Pt-LIFE), in the rat sciatic nerve. For both electrode types they found functional deficits (significantly longer latency) in the implanted nerve after 30 days, but recovery after 60 and 90 days. However, in some cases, significant reduction in amplitude of the compound muscle action potential and compound nerve action potential lasted for the entire duration of the study (90 days for Pt-LIFE electrodes and 30 and 60 days for tf-LIFE electrodes) [56]. Rossini et al. observed a steady increase in threshold using thin-film based intrafascicular electrodes (tf-LIFE4) in human median and ulnar nerves until stimulation at a safe charge level became impossible [10]. They attributed this to fibrotic tissue reaction and accommodation effects. There is at present no report on chronic use of intraneural electrodes in humans. However, the USEA and LIFEs have been used successfully in short-term (less than a month) experiments in humans [7–9, 12, 14].

Active safety – Stimulation parameters

Stimulation parameters must be selected carefully, considering electrode corrosion and tissue damage caused by passage of electric charges, as well as physiologic aspects such as stimulation efficiency and tolerance to the therapy. Generally, controlled current pulses are preferred over controlled voltage pulses, although some early attempts were made with controlled voltage stimuli [57]. As long as they do not saturate, current controlled stimulators are immune to variations in electrode impedance. Parameters

2. Safety of long-term electrical peripheral nerve stimulation



discussed here include charge injection, pulse amplitude, pulse width, pulse shape (including phase duration, separation, and phase ratio of bi-phasic pulses), pulse frequency, train rate, train duration (=‘ON’ period), stimulus cycle (=‘ON’ + ‘OFF’) period, percentage of effective stimulation time, stimulation application time, and treatment duration. A common bi-phasic stimulus pulse is displayed in Fig. 2, and a summary of parameters, labels, and units used in this work can be found in Tables 2 and 3.

Table 2 Standard stimulation parameters

Label	Parameter	Unit
A	Electrode surface area	cm ²
D	Duration of stimulating phase of a stimulus pulse	µs
D'	Duration of reversal phase of a stimulus pulse ^a	µs
F	Stimulation pulse frequency	Hz
I	Current of stimulating phase	µA
I'	Current of reversal phase ^a	µA
N	Number of pulses per train	Unitless
R	Train Rate	Hz
w	Inter-phase delay ^a	µs
P	Total application time (sum of the ‘ON’ and ‘OFF’ periods) per uninterrupted treatment duration	Hours
S	Effective stimulation time (= sum of the ‘ON’ periods) per uninterrupted treatment duration	Hours
Y	Treatment duration/Implantation Time	days OR months OR years

^a if applicable

Excitable cells such as nerve or muscle cells can be activated by electric current inducing depolarization (i.e., a reduction or even inversion of the resting voltage across the cell membrane). Upon reaching a given threshold, the depolarisation triggers self-reinforcing mechanisms. The result is an action potential that is a short-duration membrane potential inversion able to induce the same phenomenon in neighbouring membrane regions. The action potential event thus propagates along the excitable fiber. Due to the electrical capacitance of cell membranes, the stimulation pulse duration affects the current required to reach the threshold voltage for membrane activation. Therefore, excitability of a tissue is commonly characterized by a strength-duration curve, representing the current amplitude required to reach a threshold with pulses of a given duration. Two parameters characterize this curve: the rheobase current and the chronaxie time. The rheobase is defined as the minimal current required to evoke an action potential with an infinitely long duration pulse, and the chronaxie is the minimum duration to evoke an action potential with pulse intensities of twice the rheobase current [58]. Excitation properties of different tissues are thus quantified by their specific strength-duration characteristic first experimentally derived in the early 1900’s by Weiss [59] and Lapicque [60]. The non-linearity of these curves explains why electric charge injection required to reach threshold tends to increase with pulse duration, especially above the chronaxie value.

Charge

The level of electrode corrosion, an irreversible reaction, is primarily related to charges faradaically and irreversibly transferred. For different electrode materials, charge

Table 3 Derived stimulation Parameters

Label	Derivation	Parameter	Unit
c	I/I'	Amplitude of stimulating and reversal phase ratio	unitless
O	S/P	Percentage of effective stimulation time	%
Q	I · D	Charge of stimulating phase	nC
QD	(I · D)/A	Charge of stimulating phase per unit area	nC/cm ²
T	S/P	Train duration	s
wF	F · O	Weighted frequency of effective stimulation	Hz

injection limits were defined by Robblee and Rose based on the reversibility of the resulting processes [61]. However, relationships between stimulation pulse parameters and tissue damage are more obscure. McCreery et al. reported similar levels of neural damage to a cat's cortex for faradaic and capacitive electrodes [62], but noted that their stimulus waveform was ideal for the faradaic electrodes used.

Safety suggestions based on charge injection per phase (pulse amplitude times pulse width per phase) and charge density (pulse amplitude times pulse width per phase over electrode surface area) have been reported in various contexts in the past [4, 63–65]. Shannon derived a model for safe stimulation [65] largely based on experimental data by McCreery et al. [64]. He defined the boundary for safe stimulation with the equation as:

$$\log(QD) = k - \log(Q)$$

where QD is the charge density per phase in nC/cm²/phase, Q is charge per phase in nC/phase, and k should be selected between 1.5 and 2.0 [65], with a k-value of 1.5 to 1.8 being most common [4]. Breaking down this equation, a k-value of 1 would result in charges strictly proportional to the electrode area, whereas a k-value of 2 would result in charge strictly proportional to the electrode perimeter. The safe current limit is thus not strictly proportional to the area, as often implied by using expressions of current or charge/unit area. The electrode perimeter is often a better normalization reference but comparing limits for electrodes of different sizes remains questionable. This issue results from the 'edge effect': the non-uniform current distribution at the surface of an electrode. This geometrical problem has been discussed in several publications [66–74].

Geometric factors not only involve the electrodes but also the structure of the tissue being stimulated. Stimulating nerve fibers that are activated at the nodes of Ranvier cannot directly be compared with micro-electrodes directly on the axon or cell membrane. Cogan et al.

discussed the differences in stimulation thresholds based on electrode size, for instance, differences between macro- and microelectrodes [4]. The popular 30 $\mu\text{C}/\text{cm}^2$ charge density threshold considered for macroelectrodes becomes a 4 nC/phase (charge per phase) threshold when dealing with microelectrodes, that is when electrode surface area can be neglected for sufficiently small surfaces. Maximal current or charge density cannot be based solely on so-called reference values unless all other conditions are equal, which is rarely the case. It is also important to point out that most recommendations have been established for brain stimulation while the corresponding literature about peripheral nerves remains scarce.

Duration

The safety of acute and chronic peripheral nerve stimulation has been demonstrated in animals and humans for pulse durations from 1 to 300 μs for the purpose of motor function and sensory feedback [43, 44, 75] (see Table 4). Longer pulse durations up to 500 μs have been reported in chronic vagus nerve stimulation without signs that raised safety concerns [76]. In regards to biostability, Mortimer et al. observed an increased rate of electrode failure with longer pulse durations from 200 μs to 500 μs , and associated this observation with electrode corrosion [77]. Similarly, Merrill et al. noted that a narrow pulse is desirable to decrease occurrence of electrochemical reactions, and therefore reduce electrode degradation [2]. These findings indicate that when technically feasible, pulses of short duration minimize charge displacements and therefore corrosion.

Earlier publications have suggested the use of stimuli in the range of 50 to 1000 μs [78], or starting as low as 10 μs [38]. The pulse durations mentioned in the modern peripheral nerve stimulation literature are generally below 300 μs (see Table 4). Strength-duration curves show that when considering charge injection, pulses of shorter duration are more effective in eliciting tissue responses. Crago et al. found that narrow, high amplitude pulses are more effective (with less charge) than long, low amplitude pulses for intramuscular and neural stimulation in rats and cats [79]. Butterwick et al. obtained similar results stimulating chick chorioallantoic membranes and retinas, observing a decrease in threshold current density proportional to increasing pulse duration [80]. Similarly, Prado-Guitierrez et al. compared pulse widths of 104 μs and 208 μs in stimulation of the cochlea in guinea pigs [81]. They noted a decrease in current level required for the longer pulse duration, however, this decrease was not proportional to the delivered charge, and therefore longer pulses were deemed less efficient in terms of injected charge. These findings are explained by the non-linearity

Table 4 Examples of stimulation parameters in literature

Publication	Subjects	Electrode type	Stimulation/Recording	Electrode Placement	Treatment Duration (Y)	Purpose of Stimulation	Stimulation Parameters													
							Charge of Stimulating Phase (Q)	Current of Stimulating Phase (I)	Duration of Stimulating Phase (D)	Stimulation Frequency (F)	Train Duration (T)	Effective Stimulation Time per Day (S)	Potential Stimulation Time per Day (P)	Percentage of Effective Stimulation (O)	Waveform Shape	Polarity	Symmetry	InterPhase Delay (w)		
Clippinger et al. [57]	A	Cuff	S	M	< 2 y	S	-	<	-	0-100	-	-	-	-	-	-	-	-	-	-
Anani et al. [97]	AB	Needle	S	M, R	< 1 d	S	< 200	250-2600	30-250	2.5-160	1	-	20	-	Rect.	M	-	-	-	-
Walker et al. [115]	A	Cuff	S	M	3 y	S	-	<	20-640	0-90	-	2	24	8.3	-	-	-	-	-	-
Anani and Körner [116]	AB	Needle	S	forearm	< 1 d	S	-	b	200	10-80	120	-	-	-	Rect.	a	-	-	-	-
Anani and Körner [116]	A	Needle	S	M, R, U	< 1 d	S	40-300	400-3000	100	10-80	-	-	3-4	-	Rect.	a	-	-	-	-
Ochoa and Torebjörk [95]	AB	Needle	S, R	M, U	< 1 d	S	-	<	250	1-300	2	-	-	3-6	Rect.	M	-	-	-	-
Dhillon et al. [8]	A	LIFE	S, R	M, U, P	< 1 m	S	< 50	< 200	250	10-800	0.5	-	-	-	Rect.	M, B	A, S	-	-	-
Dhillon and Horch [7]	A	LIFE	S, R	M	< 1 m	S	-	b	300	10-500	0.5	-	-	-	-	-	-	-	-	-
Dhillon et al. [9]	A	LIFE	S, R	M	< 1 m	S	< 60	1-200	300	10-510	0.5	-	-	-	-	B	-	-	-	-
Rossini et al. [10]	A	TF-LIFE4	S, R	M, U	< 1 m	S	< 3	10-100	10-300	10-500	0.3-0.5	-	-	-	Rect.	-	-	-	-	-
Horch et al. [11]	A	LIFE	S	M, U	< 2 w	S	-	b	290	20-200	-	-	-	-	-	B	-	-	-	75
Clark et al. [12]	A	USEA	S, R	M, U	< 1 m	S	2-24	10-12	200	200	0.2	-	-	-	-	-	-	-	-	-
Ortiz-Catalan et al. [18]	A	Cuff	S	U	20 m	S	-	100-180	-	8-30	-	-	-	-	-	B	-	-	-	-
Raspopovic et al. [13]	A	TIME	S	M, U	< 1 m	S	< 24	240	100	50	0.5	-	-	-	Rect.	B	-	-	-	-
Tan et al. [17]	A	FINE	S	M, R, U	16 m & 24 m	S	-	< 2000	20-167	1-1000	< 60	-	4-6	-	Rect	B	A	-	-	-
Davis et al. [14]	A	USEA	S, R	M, U	< 1 m	S	0.2-20	1-100	200	1-320	0.2-60	-	2	-	-	B	-	-	-	100
Graczyk et al. [19]	A	FINE	S	M, R, U	3 y & 4 y	S	-	b	< 255	12.5-166	1-5	-	-	-	Rect.	B	-	-	-	-
Oddo et al. [15]	A	TIME	S	M	< 1 m	S	16	160	100	-	-	-	-	-	-	-	-	-	-	-
Schiefer et al. [21]	A	FINE	S	M, R, U	2 y & 3 y	S	-	-	255	10-125	-	-	5-6	-	-	B	-	-	-	-
Massini et al. [20]	A	Cuff	S	U	4 y	S	-	-	-	< 30	-	-	-	-	Rect.	B	A	-	-	50

Electrical Stimulation for Sensory Feedback

Table 4 Examples of stimulation parameters in literature (Continued)

Publication	Subjects	Electrode type	Stimulation/Recording	Electrode Placement	Treatment Duration (Y)	Purpose of Stimulation	Stimulation Parameters															
							Charge of Stimulating Phase (Q)	Current of Stimulating Phase (I)	Duration of Stimulating Phase (D)	Stimulation Frequency (F)	Train Duration (T)	Effective Stimulation Time per Day (S)	Potential Stimulation Time per Day (P)	Percentage of Effective Stimulation (O)	Waveform Shape	Polarity	Symmetry	Inter-Phase Delay (w)				
Ortiz-Catalan et al. [22]	A	Cuff	S	U	4 y	S	-	-	-	-	-	-	-	-	-	-	-	-	-	-	-	
Wendelken et al. [16]	A	Cuff	S, R	M, U	4–5 w	S	< 24	< 120	200	< 200	-	-	1–6	-	-	-	-	B	-	-	100	
Graczyk et al. [114]	A	FINE	S	M, R, U	5 y	S	-	300	< 255	25–299	< 3 min	-	< 6	-	-	-	-	Rect.	B	-	-	
Electrical Stimulation for Motor Function, Pain Relief, or other purposes																						
Nashold et al. [39]	CP	Cuff, Burton	S	M, R, S, U	< 11 y	O	-	ε	300	25–100	-	-	-	-	-	-	-	B	-	-	-	
Waters et al. [6]	P	Cuff	S	P	< 12 y	M	-	ε	200	33	-	-	-	-	-	-	-	Rect.	-	-	-	
Ben-Menachem et al. [83]	E	Cuff	S	V	14 w	O	-	250–3000	130–500	1–50	30–90	-	-	5–23	-	-	-	-	-	-	-	
Eleftheriades et al. [5]	Q	Ribbon	S	Ph	< 18 y	M	15–690	100–4600	150	7.2–8.3	0.9–1.3	0.016–0.48	8–12	0.2–0.4	-	-	-	-	-	-	-	
Vandorinck et al. [117]	Ul	Needle	S	T	< 1 d	O	4000	0–20000	200	20	-	0.5	100?	-	-	-	-	-	-	-	-	
Fisher et al. [93]	SCI	Cuff	S	F	3 y	M	160–420	800–2100	200	20	760	-	-	-	-	-	-	B	-	-	-	
Abdellaoui et al. [118]	COPD	T	S	-	-	-	6000–18800	15000–47000	400	35	3600	1	1	100	Rect.	B	S	-	-	-	-	
Christie et al. [26]	A, SCI	Cuff	S	A, F, Fl, LT, Mu, R, Su, Th, T	< 11 y	M, S	-	100–20000	1–255	12.5–100	-	-	-	-	-	-	-	B	-	-	-	

Subjects: AB Able-bodied, A Amputee, COPD Chronic obstructive pulmonary disease, CP Chronic pain due to peripheral nerve injury, P Centrally paralyzed ankle dorsiflexor muscle, Q Quadriplegia, SCI Spinal cord injury, Ul Urge incontinence
 Electrode types: Cuff, LIFE longitudinal intrafascicular electrode, Needle, Ribbon, f-LIFE^a thin film longitudinal intrafascicular multielectrode, T transcutaneous electrode, TIME transversal intrafascicular multichannel electrode, USEA Utah Slanted Electrode Array
 S Stimulation, R Recording
 Electrode Placement: A axillary, F femoral, Fl fibular, LT long thoracic, M median, Mu musculocutaneous, P peroneal, Ph phrenic, R radial, S sciatic, Su suprascapular, Th thoracodorsal, T tibial, U ulnar
 Purpose of Stimulation: M motor function, O other, S sensory feedback
 Stimulation Parameters: see Tables 1 and 2
 Waveform: Shape: Rect Rectangular
 Polarity: M Monophasic, B Biphasic
 Symmetry: S Symmetric, A Asymmetric
^a - continuous pattern
^b - individually determined, no specification
^c - voltage modulation

of the strength-duration relationship as described early on by Lopicque [60].

Modification of the pulse duration can allow for spatial selectivity and steeper recruitment curves [75]. In the case of eliciting somatosensory perception via peripheral nerve stimulation, Tan et al. found that the quality of a sensation can be altered by pulse width modulation [17], and more recently, Graczyk et al. documented the sensory correlates of varying pulse width and frequency [19]. The effect of quality, location, and intensity of elicited percepts when stimulating afferent fibers by varying pulse width in comparison to pulse amplitude have yet to be adequately documented.

Amplitude

Pulse amplitudes are highly influenced by the electrode placement, as larger target distances require larger stimulation currents [82]. Therefore, extrafascicular electrodes are generally operated at higher amplitudes than their intrafascicular counterparts. Furthermore, a nerve with a larger diameter naturally requires higher amplitudes for the recruitment of all its fibers. Amplitudes of up to 3100 μA have been used safely for stimulation of cat sciatic nerves [45]. In humans, Christie et al. and Vandoninck et al. applied amplitudes of up to 20 mA with cuff and needle electrodes to the fibular and tibial nerves, respectively. Ben-Menachem et al. stimulated the vagus nerve with amplitudes up to 3 mA using cuff electrodes [83]. For intrafascicular electrodes, maximal amplitudes usually lie in the range of 10 to 300 μA for motor and sensory nerves (see Table 4). In regards to safety, Agnew et al. suggested scaling damaging threshold as the ratio to the smallest pulse amplitude required for full recruitment of the alpha component of the compound action potential in the same individual [44].

Overall, one must keep in mind the safety limits of pulse width and amplitude both independently and in conjunction. This is essential during experiment design and clinical applications, to reduce unnecessary risks and optimize efficacy of energy consumption.

Pulse waveform

Waveform affects both physiological response and safety aspects of nerve stimulation. Pulses can vary in polarity, shape, symmetry, phases, and presence or absence of an interphase delay. In a recent review on restoration of somatosensory feedback via stimulation of peripheral nerves, Pasluosta et al. provided a thorough overview of different waveforms used in the field [84].

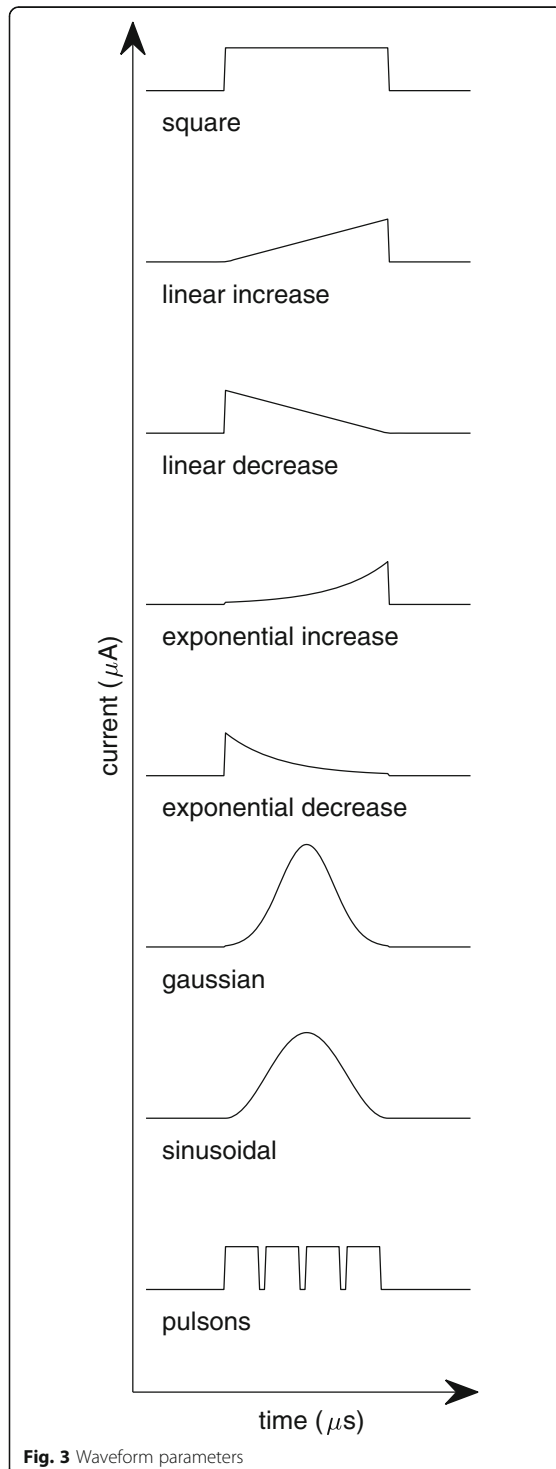
A traditional safety restriction placed on a stimulus waveform in order to prevent electro-chemical damage is a biphasic, asymmetric, charge-balanced waveform, first

introduced by Lilly et al. [85], and commonly referred to as the 'Lilly pulse'. Charge-balanced, or at least biphasic, waveforms are now commonly used (see Table 4) in order to limit any electro-chemical change [77, 86]. In terms of electrode corrosion, however, slightly unbalanced biphasic pulses might be advantageous [2, 77]. In this case, careful consideration must be given to the passive recovery between stimuli (the electrode potential recovery through the inactive stimulator output impedance).

Anodic first pulses have been used in some cases, but cathodic first pulses are the more common practice. The cathodic phase is intended to activate the excitable membrane while the anodic phase is supposed to reverse chemical processes that took place during the initial cathodic phase.

Stimulus shape parameters described here correspond to square pulses, because this shape is the most common waveform used to date. Due to the simplicity of generating square pulses, studies were traditionally conducted with this pulse shape. Further work exploring different waveforms is underway (see Fig. 3), however it is mostly limited to computer simulations at present. Non-rectangular waveforms may be less or more effective in eliciting physiological responses. Wessale et al. stimulated human subjects with surface electrodes to examine the effect of rectangular versus exponential pulses [87]. They found that rectangular pulses require slightly lower currents to reach threshold. It was hypothesized that this effect resulted from the phenomenon of accommodation, which entails an elevation of the threshold with slowly rising stimulus slopes. More recently, Sahin and Tie compared linear as well as exponential increase and decrease with rectangular, gaussian and sinusoidal waveforms. Using computational models of nerve membrane potentials, they found the chronaxie to be longer with all non-rectangular pulses. The linear, gaussian and exponential decrease waveforms were most effective in terms of charge injection and lowest threshold charge [88]. Wonsarnpigoon et al. evaluated different waveforms in terms of energy, charge, and power optimization by computational models and in vivo experiments. None of the waveforms—square, rising ramp, rising exponential and decaying exponential—were optimal in terms of all three parameters evaluated. All the reports above suggest that the strength-duration curve can vary depending on the stimulation waveform [89].

Gorman and Mortimer compared square and exponential decay waveforms for the reversal phase and found exponential decay to be more effective in terms of charge injection, as the reversal effect of the exponential decay waveform was lower. A completely novel approach was introduced by Qing et al. suggesting the use of short bursts called pulsons to optimize stimulation in terms of charge required to reach threshold and selectivity [90].



Inter-phase delay

The inter-phase delay in biphasic pulses is an essential factor, especially when stimulating close to the threshold required for generating action potentials. This delay duration is selected to 1) be long enough to minimize the stimulation threshold, while 2) still being short enough to maintain the anticorrosive effect of the charge recovery phase.

Van den Honert and Mortimer found that introducing an inter-phase delay can lower the stimulation threshold [91]. They observed that up to $100\ \mu\text{s}$ inter-phase duration and amplitude of the recovery phase influenced the degree to which an action potential could be abolished (annihilated after initiation). Gorman and Mortimer confirmed these results, observing steeper recruitment curves (stimulus current vs normalized force) and lower threshold currents with increasing interphase delay [75]. Similarly, Prado-Guitierrez et al. observed that an increase of the inter-phase delay from $8\ \mu\text{s}$ to $58\ \mu\text{s}$ evoked larger compound action potentials, and auditory brain stem responses, when stimulating the auditory nerve in guinea pigs [81]. In early stimulation protocols, inter-phase delays of up to $400\ \mu\text{s}$ were inserted between stimulating and reversal phases [45]. However, little difference between monophasic and biphasic stimuli was noted for delays larger than $80\ \mu\text{s}$, indicating that the reversing phase has no effect on abolishing action potentials if the inter-phase delay is longer than $80\ \mu\text{s}$. On the other hand, Merrill et al. recommend the introduction of an inter-phase delay smaller than $100\ \mu\text{s}$ in order to limit electrode corrosion [2]. Therefore, an inter-phase delay of about $80\text{--}100\ \mu\text{s}$ can offer an efficient way to reduce threshold currents in biphasic pulses, while still ensuring that the recovery phase starts in time to reverse the electrochemical reactions.

Frequency

Another point often overlooked is that parameters such as frequency and percentage of effective stimulation time can be damaging by physiologic functional mechanisms. In other words, high frequency pulses can impose an unacceptable level of activity to physiological structures. The resulting damage can be reversible or not and independent of the severity of the overload. Agnew et al. first noted the relevance of pulse frequency when stimulating the peroneal nerve in cats [44]. Their results showed no neural damage after continuous stimulation at $20\ \text{Hz}$ for $16\ \text{h}$. However, with otherwise identical parameters, a frequency of $50\ \text{Hz}$ resulted in neural damage. Later, McCreery et al. performed more thorough studies on the frequency parameter stimulating the sciatic nerve in cats [92]. For all tested degrees of fiber recruitment, a frequency of $20\ \text{Hz}$ proved to be safe, whereas with

increasing frequency (50 and 100 Hz) even pulses with smaller currents, and therefore only partial fiber recruitment, resulted in neural damage. McCreery et al. also highlighted the importance of the percentage of 'effective stimulation time' in relation to the choice of frequency (further discussed below). In agreement with these findings, Waters et al. safely applied stimuli with a frequency of 33 Hz for a period of up to 12 years to the human peroneal nerve [6], Ben-Menachem et al. used a frequency of typically 30 Hz for 14 weeks in human vagus nerve stimulation [83], Eleftheriades et al. applied frequencies of 7.2–8.3 Hz over periods up to 18 years in human phrenic nerves [5], and Fisher et al. stimulated the human femoral nerve with 20 Hz for 3 years [93]. The relatively low frequency tolerance found in the peripheral nerves does not seem to apply as severely to the central nervous system. In stimulation of the cochlear nucleus of guinea pigs, McCreery et al. showed that frequencies up to 100 Hz caused no damage nor stimulation-induced depression of neuronal excitability (SIDNE) after 7 h of continuous stimulation while higher frequencies of 250 and 500 Hz were damaging [94]. Kim et al. stimulated the phrenic nerve of dogs with frequencies of 7 and 35 Hz over periods up to 52 weeks and noted only minimal neural damage, which was presumed to be caused by mechanical restriction rather than the electrical stimulation [43].

Intensity and quality of referred sensations can be encoded by frequency modulation in direct peripheral nerve stimulation [19]. The range of frequencies used in such application has been wide, ranging from up to 300 Hz in initial experiments [95] to 500 Hz in some recent studies [7–9]. However, these experiments were acute and permanent nerve damage was not evaluated although arguably negligible owing to the short duration of the study and experimental sessions. As lower stimulation frequencies are sufficient for other applications (see Table 4), supporting evidence for the safety of long-term electrical stimulation of peripheral nerves only exists for frequencies below 30 Hz at present.

Percentage of effective stimulation time

The term 'duty cycle' has been used in the past to describe the percentage of 'ON' versus 'OFF' stimulation time [44, 94, 96]. For instance, stimulation of 5 s ('ON'), followed by a pause of 5 s ('OFF') before engaging in stimulation again was described as a 50% duty cycle by dividing the 'ON' time (5 s) by the overall time (10 s). However, in engineering, the 'duty cycle' is usually defined over a single pulse duration ($D + D'$), rather than to the total period of stimulation as aforementioned. For instance, a duty cycle of 50% would normally imply that a pulse with a period of 1.0 s is active for 0.5 s, regardless of how long a stimulation is being delivered. In other

words, a 100% duty cycle would be equivalent to DC stimulation (or to a pulse duration equal to the pulse period), and 0% duty cycle would be equivalent to no or 'OFF' stimulation. In order to avoid ambiguity between these two definitions, in this article we use the term 'percentage of effective stimulation time' to refer to the former ($O=S/P$). Train rate (R), is a equivalent to stimulation pulse frequency (F) when the total application time is equivalent to the effective stimulation time ($S=P$), see Tables 2 and 3.

It has been suggested that by decreasing the percentage of effective stimulation time one can safely increase other stimulation parameters. Agnew et al. showed that with 50% effective stimulation time, it is possible to stimulate a cat peroneal nerve at higher frequencies than 50 Hz, and for a period of 16 h, while causing considerably less damage to the nerve than at 100% effective stimulation time [44]. Tykocinski et al. observed a smaller decrease in excitability and faster recovery after stimulation of the auditory nerve in guinea pigs when using 50% effective stimulation time compared to continuous stimulation [96].

The impact of the percentage of effective stimulation time in human peripheral nerve stimulation is rarely documented in the literature for both acute and chronic applications. In an early acute study, Anani et al. stimulated median and radial nerves of able-bodied subjects with an effective stimulation time of 17%. Although threshold changes made an up-regulation of parameters necessary in some cases, no indication of permanent damage was reported [97]. Eleftheriades et al. stimulated the phrenic nerve for 8 to 12 h per day with 17 to 26% of effective stimulation time and found constant threshold currents over time periods of up to 18 years [5]. Similarly, vagus nerve stimulation is commonly applied with low percentages of effective stimulation time of 9–27% [98].

McCreery et al. suggested the use of a parameter they called 'average frequency', equal to stimulus frequency times the percentage of effective stimulation time, as a means of predicting SIDNE, which is considered an early stage of neural damage [94]. When stimulating the cochlear nucleus in cats for 7 h at higher overall average frequencies above 100 Hz, they noted an increase in the threshold of the evoked response proportional to the average frequency, indicating this parameter is more meaningful than either frequency or percentage of effective stimulation time alone. In their study, only one frequency at a time was employed, followed by a period of no stimulation. Therefore, speaking of an 'average' could be misleading since an average normally corresponds to variable values over the number of values. Consequently, the term 'weighted frequency of effective stimulation time' is proposed as an alternative to 'average frequency' (see Tables 2 and 3). The pioneering work of McCreery et al. has not been continued nor expanded upon to other frequencies or neural tissues.

Stimulation application time and treatment duration

In this article, the stimulation application time is considered as the time per day during which stimulation is active, whereas treatment duration is the overall duration an electrode was implanted and active. As discussed previously, the length of stimulation application has been shown to influence the degree of induced neural damage. Specifically, Agnew et al. noted that it is possible to stimulate safely with identical parameters if the duration of stimulation was decreased from 16 h to 4 h [44]. The duration of continued stimulation rarely exceeded 8 h in animal studies, making it difficult to draw conclusions on the length of time one can safely stimulate peripheral nerves based on these experiments. In human studies, stimulation application length in acute experiments is commonly below 6 h, and normally intermittent (see Table 4). Chronic but intermittent stimulation had been reported successful for therapy periods up to 18 years [5]. However, information on the safety of chronic and uninterrupted peripheral nerve stimulation is absent, and yet needed for applications such as restoring proprioception and sensory feedback capabilities of limb prostheses.

Transferability

Due to the lack of experimental data on safety restrictions specific to human peripheral nerve stimulation, researchers often extrapolate from findings about other nerves and/or animal studies. A brief review of the appropriateness of such a practice is given in this section.

Transferability between species

Ethical considerations often prevent testing safety limitations in humans. Consequently, a large part of the literature and of our knowledge about neural stimulation is based on animal studies mostly conducted in the 1980s and 1990s [43–45, 62–64, 75, 92, 94, 96, 99, 100]. Biostability of electrodes as well as passive harmlessness are similar in animals and humans. In an early review, Agnew and McCreery argued that when extrapolating stimulation parameters from animal studies to humans, physiological parameters such as diameter of the stimulated nerve should be considered above other factors [1].

Transferability between species is generally admitted for passive and active aspects of biostability and passive aspects of harmlessness. However, there are sometimes diverging reactions to electrical stimulation due to functional physiological differences as well as easily identifiable parameters such as conduction velocity, fiber diameter, axon count, or myelination. Transferability should be considered with caution when these parameters diverge too significantly.

Transferability between tissue types

Studies on stimulation of the peripheral nervous system are not always a suitable reference for stimulation of the central nervous system or muscle tissue, and vice versa. However, passive and active biostability are expected to show some similarity between various tissue types, and are highly comparable if the temperature and composition of the surroundings are similar.

Previous reviews have highlighted that physiological differences between the brain and peripheral nerves explain the differences in the range of electrical stimulation parameters used in both situations [25, 101]. In transcutaneous peripheral stimulation, pulse durations observed in the literature are longer (up to 400 μ s) than those given for implanted electrodes (see Table 4). Pulse frequencies used in skin surface stimulation are generally in the range of 8 to 100 Hz [102], and therefore below frequency ranges commonly observed in neural stimulation (see Table 4). Use of higher frequencies of 100 Hz and 200 Hz has shown to be viable for stimulation of the auditory nerve [96].

In summary, physiological characteristic differences must be considered when comparing active harmlessness, whereas passive harmlessness and biostability characteristics in general are expected to be relatively similar.

Diversity in the peripheral nervous system

Stimulation safety limits cannot be applied as a global concept to neural tissue due to the diversity of cells forming it [103]. Peripheral nerves have a variety of fibers with different physiology and function, as well as Schwann cells, blood vessels, and various supporting cells [42, 104–106]. All these cells are potentially sensitive to electrostimulation in different ways leading to diverse consequences.

Neural stimulation has more effects than the mere initiation of an 'action potential' transmitted to higher physiological structures. Some of these effects could be referred to as trophic effects of neural stimulation. Collateral sprouting in motor nerves and regeneration in sensory nerves are modulated by the neural activity [107–110]. Similar mechanisms probably exist throughout the nervous system and some forms of cerebral plasticity can be interpreted in this context [111]. However, the underlying mechanisms remain poorly known. The SIDNE phenomenon and the demonstration that 'overstimulation' can kill a nerve [44] can also be considered as a trophic mechanism [112]. Although this has never been demonstrated, it would seem logical that safe stimulation should not impose much more activation to the nerve than its functional physiological level. This limit can vary between different nerves and should

thus be investigated for each neural structure and nerve type separately.

Maximal tolerated stimulation pulse frequencies vary for different neural structures as demonstrated in a number of publications including the relatively low stimulus frequency tolerance of motor nerves when compared to examples in the central nervous system [44, 65, 92]. Not only the frequency but the effect of each stimulus parameters must be considered. There is thus a need for specific chronic safety studies in various neural structures considering all stimulus parameters. These studies still leave open the question of validity for humans. Numerous studies have already been published including several reviews [1, 4]. Unfortunately, the available data still fall short of covering the topic in any systematic way, and it must be pointed out that at best, the limits proposed today are mere extrapolations.

Classification of neural damage

Evidently, knowledge about the safety limits of stimulation parameters is rather limited, especially for peripheral nerves in humans. Although electrode design has significantly improved and conditions for passive biostability and harmlessness are generally agreed upon, a high degree of uncertainty about the effects of electrical stimulation remains.

Inflammation is always present after chronic implantation. This can be inactive, leaving fibrous tissue which can for example shield the nerve fibers from the stimulation current. Resulting variations in impedances and stimulation thresholds seem to stabilize 8 weeks post implantation [51]. If the inflammatory reaction remains active, various molecular factors that can directly affect the functionality of neural tissue are being released.

A major issue in comparing different studies is the lack of a common classification of reversible and irreversible neural damage. Until now, neural damage has been evaluated in terms of evoked action potential and functional performance in living subjects, as well as by post-mortem histology. Local damage in peripheral nerves can occur through several mechanisms, resulting mainly in axonal degeneration and demyelination. These damages could be reversible if no further stimulation is applied [54, 113].

Several techniques have been used to evaluate the degree of damage. Agnew et al. recorded the amplitude of the alpha component of the compound action potential at different current intensities before and after stimulation of the peroneal nerve in cats [44]. However, no direct correlation was found between amplitude changes and the percentage of degenerated axons. McCreery et al. used a similar amplitude-based principle to evaluate SIDNE in stimulation of the cat's posteroventral cochlear nucleus. They showed a correlation between the level of

SIDNE and the pulse frequency and stimulation duration, respectively, but no injury could be detected on histological evaluation [94]. Adaptation mechanisms taking place during electrical stimulation of peripheral nerves as described by Graczyk et al. [114] may also have an effect on what McCreery et al. described as SIDNE. Potential connections must be explored in the future. Demyelination should also result in slowing of the nerve conduction velocity if the affected nerve section is long enough for the measurement to be performed.

Peripheral nerves, like brain tissue, contain not only various types of axons but also other important cells such as the Schwann cells, immune cells, and vascular structures with blood-nerve barrier, all in an organized anatomical arrangement. Considering this complexity, it is perhaps not surprising that different evaluation parameters yield different results. A study on the effect of the individual stimulation parameters on specific physiological characteristics is necessary to yield a transferable understanding of damaging limits. In this context, the functional significance and reversibility of any observed change must also be considered, because tissue physiology participates actively in the implantation process. There is therefore still a need for better discrimination and classification of the various actors and targets of peripheral nerve stimulation safety limits.

Conclusion

In this work, we summarized current knowledge on safe stimulation protocols in peripheral nerves and discussed relevant concerns. Currently, extraneural electrodes have proven safe for chronic applications while invasiveness and long-term stability of intraneural electrode remain challenging for permanent implantation. Safety limits of stimulation parameters are still predominantly described in terms of electric charge. The popular Shannon equation may provide some guidance toward elucidating safety limits, however the same equation points to the fact that acceptable limits cannot be normalized to the electrode contact size. Consequently, normative data cannot be applied to electrodes of different sizes. Regarding pulse width and amplitude, short pulses require lower electric charges to elicit action potentials, and therefore short pulses should be preferred whenever the necessary higher current amplitudes are technically feasible. The only available study about the allowable stimulation frequency in chronic peripheral nerve stimulation suggests that 50 Hz is a maximal limit. However, with a reduced percentage of effective stimulation time, higher frequencies might still be safe as well. Long-term studies should further investigate this issue. Furthermore, the use of different pulse shapes could improve efficiency as suggested by computational models and in-vitro

experiments, but in-vivo comparative studies are still lacking. Direct individual functional monitoring, as suggested by Agnew et al. in 1989, could offer a useful alternative to published safety limit values for the clinical determination of electric stimulation parameters [44], and future safety studies should consider the diversity of cells in peripheral nerves and how these are affected by electrical stimulation. The reactions of the different neural structures to an implant and to electrical stimulation can cause structural and functional changes over time. In addition, the therapeutic use of neuromodulation can induce phenomena such as central plasticity and peripheral axonal growth or collateral compensation. Time is thus an essential parameter and there is a need for chronic follow up studies.

A major limitation when performing this review was the lack of systematic documentation of stimulation parameters in the literature. We hope this paper will help drawing more attention to these aspects and help to standardize the reporting of stimulation protocols (Tables 2 and 3). The aim of such a parameter list is to allow for effective comparison and meta-analysis that draw more meaningful and broader conclusions about the safety aspects of neural stimulation.

Acknowledgements

We thank our funding sources below.

Funding

This work was funded by the Stiftelsen Promobilia, VINNOVA, and the European Commission (H2020 DeTOP and FLAG-ERA GRAFIN projects).

Availability of data and materials

Not applicable.

Authors' contributions

CG drafted manuscript; CG, JD, and MOC edited and revised manuscript; CG, JD, and MOC approved final version of manuscript.

Ethics approval and consent to participate

Not applicable.

Consent for publication

Not applicable.

Competing interests

CG and JD declare having no competing interests. MOC was partially funded by Integrum AB, a for-profit organization, which is developing bone-anchored limb prosthesis with neural control.

Publisher's Note

Springer Nature remains neutral with regard to jurisdictional claims in published maps and institutional affiliations.

Author details

¹Biomechanics and Neurorehabilitation Laboratory, Department of Electrical Engineering, Chalmers University of Technology, 41296 Gothenburg, Sweden. ²LCEN3, Department of Neurology, Institute of Neuroscience, Ghent University, C. Heymanslaan, 10, 9000 Ghent, Belgium. ³Integrum AB, Krokslätt Fabrik 50, 43137 Mölndal, Sweden.

Received: 1 August 2018 Accepted: 11 December 2018

Published online: 18 January 2019

References

1. Agnew WF, McCreery DB. Considerations for safety with chronically implanted nerve electrodes. *Epilepsia*. 1990;31:527–32.
2. Merrill DR, Bikson M, Jefferys JGR. Electrical stimulation of excitable tissue: design of efficacious and safe protocols. *J Neurosci Methods*. 2005;141:171–98.
3. Cogan SF. Neural stimulation and recording electrodes. *Annu Rev Biomed Eng*. 2008;10:275–309.
4. Cogan SF, Ludwig KA, Welle CG, Takmakov P. Tissue damage thresholds during therapeutic electrical stimulation. *J Neural Eng*. 2016;13:021001.
5. Eleftheriades JA, Quin JA, Hogan JF, Holcomb WG, Letsou GV, Chlosta WF, et al. Long-term follow-up of pacing of the conditioned diaphragm in quadriplegia. *Pacing Clin Electrophysiol*. 2002;25:897–906.
6. Waters RL, McNeal DR, Faloon W, Clifford B. Functional electrical stimulation of the peroneal nerve for hemiplegia. Long-term clinical follow-up. *J Bone Jt Surg*. 1985;67:792–3.
7. Dhillon GS, Horch KW. Direct neural sensory feedback and control of a prosthetic arm. *IEEE Trans Neural Syst Rehabil Eng*. 2005;13:468–72.
8. Dhillon GS, Lawrence SM, Hutchinson DT, Horch KW. Residual function in peripheral nerve stumps of amputees: implications for neural control of artificial limbs. *J Hand Surg Am*. 2004;29:605–15.
9. Dhillon GS, Krüger TB, Sandhu JS, Horch KW. Effects of short-term training on sensory and motor function in severed nerves of long-term human amputees. *J Neurophysiol Am Physiological Soc*. 2005;93:2625–33.
10. Rossini PM, Micera S, Benvenuto A, Carpaneto J, Cavallo G, Citi L, et al. Double nerve intraneural interface implant on a human amputee for robotic hand control. *Clin Neurophysiol*. 2010;121:777–83.
11. Horch KW, Meek S, Taylor TG, Hutchinson DT. Object discrimination with an artificial hand using electrical stimulation of peripheral tactile and proprioceptive pathways with intrafascicular electrodes. *IEEE Trans Neural Syst Rehabil Eng*. 2011;19:483–9.
12. Clark GA, Wendelken S, Page DM, Davis T, Wark HAC, Normann RA, et al. Using multiple high-count electrode arrays in human median and ulnar nerves to restore sensorimotor function after previous transradial amputation of the hand. 36th Annu Int Conf Proc IEEE Eng Med Biol Soc. 2014:1977–80. <https://ieeexplore.ieee.org/document/6944001>.
13. Raspopovic S, Capogrosso M, Petrini FM, Bonizzato M, Rigosa J, Di Pino G, et al. Restoring Natural Sensory Feedback in Real-Time Bidirectional Hand Prostheses. *Sci Transl Med*. 2014;6:222ra19.
14. Davis TS, Wark HAC, Hutchinson DT, Warren DJ, O'Neill K, Scheinblum T, et al. Restoring motor control and sensory feedback in people with upper extremity amputations using arrays of 96 microelectrodes implanted in the median and ulnar nerves. *J Neural Eng*. 2016;13:03600.
15. Oddo CM, Raspopovic S, Artoni F, Mazzoni A, Spigler G, Petrini FM, et al. Intraneural stimulation elicits discrimination of textural features by artificial fingertip in intact and amputee humans. *elife*. 2016;5:1–27.
16. Wendelken S, Page DM, Davis T, Wark HAC, Kluger DT, Duncan C, et al. Restoration of motor control and proprioceptive and cutaneous sensation in humans with prior upper-limb amputation via multiple Utah slanted electrode arrays (USEAs) implanted in residual peripheral arm nerves. *J Neuroeng Rehabil*. 2017;14:121.
17. Tan DW, Schiefer MA, Keith MW, Anderson JR, Tyler J, Tyler DJ. A neural interface provides long-term stable natural touch perception. *Sci Transl Med*. 2014;6:257ra138.
18. Ortiz-Catalan M, Håkansson B, Brånemark R. An osseointegrated human-machine gateway for long-term sensory feedback and motor control of artificial limbs. *Sci Transl Med*. 2014;6:257re6.
19. Graczyk EL, Schiefer MA, Saal HP, Delhaye BP, Bensaïda SJ, Tyler DJ. The neural basis of perceived intensity in natural and artificial touch. *Sci Transl Med*. 2016;8:362ra142.
20. Mastinu E, Doguet P, Botquin Y, Håkansson B, Ortiz-Catalan M. Embedded system for prosthetic control using implanted neuromuscular interfaces accessed via an Osseointegrated implant. *IEEE Trans Biomed Circuits Syst*. 2017;11:867–77.
21. Schiefer MA, Tan DW, Sidek SM, Tyler DJ. Sensory feedback by peripheral nerve stimulation improves task performance in individuals with upper limb loss using a myoelectric prosthesis. *J Neural Eng*. 2016;13:016001.

2. Safety of long-term electrical peripheral nerve stimulation

22. Ortiz-Catalan M, Mastinu E, Brånemark R, Håkansson B. Direct Neural Sensory Feedback and Control via Osseointegration. Cape Town: XVI World Congr Int Soc Prosthetics Orthot (ISPO); 2017.
23. Hartline DK, Colman DR. Rapid conduction and the evolution of Giant axons and myelinated fibers. *Curr Biol*. 2007;17:29–35.
24. Johansson RS, Flanagan JR. Coding and use of tactile signals from the fingertips in object manipulation tasks. *Nat Rev Neurosci*. 2009;10:345–59.
25. Kim Y, Romero-Ortega MI. Material considerations for peripheral nerve interfacing. *MRS Bull*. 2012;37:573–80.
26. Christie BP, Freeberg M, Memberg WD, Pinault GJC, Hoyen HA, Tyler DJ, et al. Long-term stability of stimulating spiral nerve cuff electrodes on human peripheral nerves. *J Neuroeng Rehabil*. 2017;14:70.
27. Tyler DJ, Durand DM. Functionally selective peripheral nerve stimulation with a flat interface nerve electrode. *IEEE Trans Neural Syst Rehabil Eng*. 2002;10:294–303.
28. Nielsen TN, Sevcencu C, Struijk JJ. Comparison of mono-, bi-, and Tripolar configurations for stimulation and recording with an Interfascicular Interface. *IEEE Trans Neural Syst Rehabil Eng*. 2014;22:88–95.
29. Badi AN, Hillman T, Shelton C, Normann RA. A technique for implantation of a 3-dimensional penetrating electrode array in the modiolar nerve of cats and humans. *Arch Otolaryngol - Head Neck Surg*. 2002;128:1019–25.
30. Bowman BR, Erickson RC. Acute and chronic implantation of coiled wire intraneural electrodes during cyclical electrical stimulation. *Ann Biomed Eng*. 1985;13:75–93.
31. Lacour SP, Fitzgerald JJ, Lago N, Tarte E, McMahon S, Fawcett J. Long Micro-Channel electrode arrays: a novel type of regenerative peripheral nerve interface. *IEEE Trans Neural Syst Rehabil Eng*. 2009;17:454–60.
32. Stieglitz T, Beutel H, Meyer J-U. A flexible, light-weight multichannel sieve electrode with integrated cables for interfacing regenerating peripheral nerves. *Sensors Actuators*. 1997;60:240–3.
33. Garde K, Keefer E, Botterman B, Galvan P, Romero-Ortega MI. Early interfaced neural activity from chronic amputated nerves. *Front Neuroeng*. 2009;2:1–11.
34. Mannard A, Stein RB, Charles D. Regeneration electrode Units : implants for recording from single peripheral nerve fibers in freely moving animals. *Science*. 2018;183:547–9.
35. Lacour SP, Atta R, Fitzgerald JJ, Blamire M, Tarte E, Fawcett J. Polyimide micro-channel arrays for peripheral nerve regenerative implants. *Sensors Actuators A Phys*. 2008;147:456–63.
36. Navarro X, Krueger TB, Lago N, Micera S, Stieglitz T, Dario P. A critical review of interfaces with the peripheral nervous system for the control of neuroprostheses and hybrid bionic systems. *J Peripher Nerv Syst*. 2005;10:229–58.
37. Ortiz-Catalan M, Brånemark R, Håkansson B, Delbeke J. On the viability of implantable electrodes for the natural control of artificial limbs: review and discussion. *Biomed Eng Online*. 2012;11:33.
38. Brummer SB, Turner MJ. Electrochemical considerations for safe electrical stimulation of the nervous system with platinum electrodes. *IEEE Trans Biomed Eng*. 1977;24:59–63.
39. Nashold BS Jr, Goldner JL, Mullen JB, Bright DS. Long-term pain control by direct peripheral-nerve stimulation. *J Bone Jt Surg*. 1982;64:1–10.
40. Anderson JM. Biological responses to materials. *Annu Rev Mater Res*. 2001; 31:81–110.
41. Rickett T, Connell S, Bastjancic J, Hegde S, Shi R. Functional and mechanical evaluation of nerve stretch injury. *J Med Syst*. 2011;35:787–93.
42. Olsson Y. Microenvironment of the peripheral nervous system under normal and pathological conditions. *Crit Rev Neurobiol*. 1990;5:265–311.
43. Kim JH, Manuelidis EE, Glenn WWL, Fukuda Y, Cole DS, Hogan JF. Light and electron microscopic studies of phrenic nerves after long-term electrical stimulation. *J Neurosurg*. 1983;58:84–91.
44. Agnew WF, McCreery DB, Yuen TGH, Bullara LA. Histologic and physiologic evaluation of electrically stimulated peripheral nerve: considerations for the selection of parameters. *Ann Biomed Eng*. 1989;17:39–60.
45. McCreery DB, Agnew WF, Yuen TGH, Bullara LA. Damage in peripheral nerve from continuous electrical stimulation: comparison of two stimulus waveforms. *Med Biol Eng Comput*. 1992;30:109–14.
46. Naples GG, Mortimer JT, Scheiner A, Sweeney JD. A spiral nerve cuff electrode for peripheral nerve stimulation. *IEEE Trans Biomed Eng*. 1988;35: 905–16.
47. Mortimer JT, Agnew WF, Horch KW, Citron P, Creasey G, Kantor C. Perspectives on new electrode Technology for Stimulating Peripheral Nerves with implantable motor prostheses. *IEEE Trans Rehabil Eng*. 1995;3: 145–54.
48. Loeb GE, Peck RA. Cuff electrodes for chronic stimulation and recording of peripheral nerve activity. *J Neurosci Methods Elsevier*. 1996;64:95–103.
49. Prodanov D, Delbeke J. Mechanical and biological interactions of implants with the brain and their impact on implant design. *Front Neurosci*. 2016;10:11.
50. Kilgore KL, Peckham PH, Keith MW, Montague FW, Hart RL, Gazdik MM, et al. Durability of implanted electrodes and leads in an upper-limb neuroprosthesis. *J Rehabil Res Dev*. 2003;40:457–68.
51. Grill WM, Mortimer JT. Stability of the input-output properties of chronically implanted multiple contact nerve cuff stimulating electrodes. *IEEE Trans Rehabil Eng*. 1998;6:364–73.
52. Grill WM, Mortimer JT. Neural and connective tissue response to long-term implantation of multiple contact nerve cuff electrodes. *J Biomed Mater Res*. 2000;50:215–26.
53. Girsch W, Koller R, Gruber H, Holle J, Liegl C, Losert U, et al. Histological assessment of nerve lesions caused by epineurial electrode application in rat sciatic nerve. *J Neurosurg*. 1991;74:636–42.
54. Larsen JO, Thomsen M, Haugland M, Sinkjær T. Degeneration and regeneration in rabbit peripheral nerve with long-term nerve cuff electrode implant: a stereological study of myelinated and unmyelinated axons. *Acta Neuropathol*. 1998;96:365–78.
55. Christensen MB, Pearce SM, Ledbetter NM, Warren DJ, Clark GA, Tresco PA. The foreign body response to the Utah Slant Electrode Array in the rat sciatic nerve. *Acta Biomater*. 2014;10:4650–60 Acta Materialia Inc.
56. Lago N, Yoshida K, Koch KP, Navarro X. Assessment of biocompatibility of chronically implanted polyimide and platinum Intrafascicular electrodes. *IEEE Trans Biomed Eng*. 2007;54:281–90.
57. Clippinger FW, Avery R, Titus BR. A sensory feedback system for an upper-limb amputation prosthesis. *Bull Prosthet Res*. 1974;10–22:247–58.
58. Lapique L. Has the muscular substance a longer chronaxie than the nervous substance? *J Physiol*. 1931;73:189–214.
59. Weiss G. Sur la possibilité de rendre comparables entre eux les appareils servant à l'excitation électrique. *Arch Ital Biol*. 1901;35:413–46.
60. Lapique L. Recherches quantitatives sur l'excitation électrique des nerfs traitée comme une polarisation. *J Physiol Pathol générale*. 1907;9:620–35.
61. Robblee LS, Rose TL. The electrochemistry of electrical stimulation. *Annu International Conf IEEE Eng Med Biol Soc*. 1990;12:1479–80.
62. McCreery DB, Agnew WF, Yuen TGH, Bullara LA. Comparison of neural damage induced by electrical stimulation with faradaic and capacitor electrodes. *Ann Biomed Eng*. 1988;16:463–81.
63. Agnew WF, Yuen TGH, McCreery DB. Morphologic changes after prolonged electrical stimulation of the cat's cortex at defined charge densities. *Exp Neurol*. 1983;79:397–411.
64. McCreery DB, Agnew WF, Yuen TGH, Bullara LA. Charge density and charge per phase as cofactors in neural injury induced by electrical stimulation. *IEEE Trans Biomed Eng*. 1990;37:996–1001.
65. Shannon RV. A model of safe levels for electrical stimulation. *IEEE Trans Biomed Eng*. 1992;39:424–6.
66. Behrend MR, Ahuja AK, Weiland JD. Dynamic Current Density of the Disk Electrode Double-Layer. *IEEE Trans Biomed Eng*. 2008;55:1056–62.
67. Cantrell DR, Inayat S, Taflove A, Ruoff RS, Troy JB. Incorporation of the electrode-electrolyte interface into finite-element models of metal microelectrodes. *J Neural Eng*. 2008;5:54–67.
68. Hudak EM, Mortimer JT, Martin HB. Platinum for neural stimulation: voltammetry considerations. *J Neural Eng*. 2010;7:026005.
69. Krasteva VT, Papazov SP. Estimation of current density distribution under electrodes for external defibrillation. *Biomed Eng Online*. 2002;1:1–13.
70. Ksienski DA. A minimum profile uniform current density electrode. *IEEE Trans Biomed Eng*. 1992;39:682–92.
71. Rubinstein JT, Spelman FA, Soma M, Suesserman MF. Current density profiles of surface mounted and recessed electrodes for neural prostheses. *IEEE Trans Biomed Eng*. 1987;34:864–75.
72. Suesserman MF, Spelman FA, Rubinstein JT. In vitro measurement and characterization of current density profiles produced by nonrecessed, simple recessed, and radially varying recessed stimulating electrodes. *IEEE Trans Biomed Eng*. 1991;38:401–8.
73. Wei XF, Grill WM. Current density distributions, field distributions and impedance analysis of segmented deep brain stimulation electrodes. *J Neural Eng*. 2005;2:139–47.

2. Safety of long-term electrical peripheral nerve stimulation

74. Wei XF, Grill WM. Analysis of high-perimeter planar electrodes for efficient neural stimulation. *Front Neuroeng.* 2009;2:1–10.
75. Gorman PH, Mortimer JT. The effect of stimulus parameters on the recruitment characteristics of direct nerve stimulation. *IEEE Trans Biomed Eng.* 1983;30:407–14.
76. DeGiorgio CM, Schachter SC, Handforth A, Salinsky M, Thompson J, Uthman B, et al. Prospective long-term study of vagus nerve stimulation for the treatment of refractory seizures. *Epilepsia.* 2000;41:1195–200.
77. Mortimer JT, Kaufman D, Roessmann U. Intramuscular electrical stimulation: tissue damage. *Ann Biomed Eng.* 1980;8:235–44.
78. Lilly JC. Injury and excitation by electric currents. In: Sheer DE, editor. *Electr Stimul brain.* Austin: University of Texas Press; 1961. p. 60–4.
79. Crago PE, Peckham PH, Mortimer JT, Van Der Meulen JP. The choice of pulse duration for chronic electrical stimulation via surface, nerve, and intramuscular electrodes. *Ann Biomed Eng.* 1974;2:252–64.
80. Butterwick A, Vankov A, Huie P, Freyvert Y, Palanker D. Tissue damage by pulsed electrical stimulation. *IEEE Trans Biomed Eng IEEE.* 2007;54:2261–7.
81. Prado-Guitierrez P, Fewster LM, Heasman JM, McKay CM, Shepherd RK. Effect of interphase gap and pulse duration on electrically evoked potentials is correlated with auditory nerve survival. *Hear Res.* 2006; 215:47–55.
82. Rattay F. Analysis of models for external stimulation of axons. *IEEE Trans Biomed Eng.* 1986;33:974–7.
83. Ben-Menachem E, Mañon-Españallat R, Ristanovic R, Wilder BJ, Stefan H, Mirza W, et al. Vagus nerve stimulation for treatment of partial seizures: 1. A controlled study of effect on seizures. *Epilepsia.* 1994;35:616–26.
84. Pasluosta C, Kiele P, Stieglitz T. Paradigms for restoration of somatosensory feedback via stimulation of the peripheral nervous system. *Clin Neurophysiol.* 2018;129:851–62.
85. Lilly JC, Hughes JR, Alvord EC, Galkin TW. Brief, noninjurious electric waveform for stimulation of the brain. *Adv Sci.* 1955;121:468–9.
86. Scheiner A, Mortimer JT, Roessmann U. Imbalanced biphasic electrical stimulation: muscle tissue damage. *Ann Biomed Eng.* 1990;18:407–25.
87. Wessale JL, Geddes LA, Ayers GM, Foster KS. Comparison of rectangular and exponential current pulses for evoking sensation. *Ann Biomed Eng.* 1992;20: 237–44.
88. Sahin M, Tie Y. Non-rectangular waveforms for neural stimulation with practical electrodes. *J Neural Eng.* 2007;4:227–33.
89. Wongsampigoon A, Woock JP, Grill WM. Efficiency analysis of waveform shape for electrical excitation of nerve fibers. *IEEE Trans Neural Syst Rehabil Eng.* 2010;18:319–28.
90. Qing KY, Ward MP, Irazoqui PP. Burst-modulated waveforms optimize electrical stimuli for charge efficiency and fiber selectivity. *IEEE Trans Neural Syst Rehabil Eng.* 2015;23:936–45.
91. Van den Honert C, Mortimer JT. The response of the myelinated nerve fiber to short duration biphasic stimulating currents. *Ann Biomed Eng.* 1979;7: 117–25.
92. McCreery DB, Agnew WF, Yuen TGH, Bullara LA. Relationship between stimulus amplitude, stimulus frequency and neural damage during electrical stimulation of sciatic nerve of cat. *Med Biol Eng Comput.* 1995;33:426–9.
93. Fisher LE, Miller ME, Bailey SN, Davis JA, Anderson JS, Rhode L, et al. Standing after spinal cord injury with four-contact nerve-cuff electrodes for quadriceps stimulation. *IEEE Trans Neural Syst Rehabil Eng.* 2008;16:473–8.
94. McCreery DB, Yuen TGH, Agnew WF, Bullara LA. A characterization of the effects on neuronal excitability due to prolonged microstimulation with chronically implanted microelectrodes. *IEEE Trans Biomed Eng.* 1997;44:931–9.
95. Ochoa J, Torebjörk E. Sensations evoked by intraneural microstimulation of single mechanoreceptor units innervating the human hand. *J Physiol.* 1983; 342:633–54.
96. Tykocinski M, Shepherd RK, Clark GM. Reduction in excitability of the auditory nerve following electrical stimulation at high stimulus rates. *Hear Res.* 1995;88:124–42.
97. Anani AB, Ikeda K, Körner LM. Human ability to discriminate various parameters in afferent electrical nerve stimulation with particular reference to prostheses sensory feedback. *Med Biol Eng Comput.* 1977;15:363–73.
98. Johnson RL, Wilson CG. A review of vagus nerve stimulation as a therapeutic intervention. *J Inflamm Res.* 2018;11:203–13.
99. Yuen TGH, Agnew WF, Bullara LA, Jacques S, McCreery DB. Histological evaluation of neural damage from electrical stimulation: considerations for the selection of parameters for clinical application. *Neurosurgery.* 1981;9: 292–9.
100. Agnew WF, McCreery DB, Yuen TGH, Bullara LA. Local anaesthetic block protects against electrically-induced damage in peripheral nerve. *J Biomed Eng.* 1990;12:301–8.
101. Weber DJ, Friesen R, Miller LE. Interfacing the somatosensory system to restore touch and proprioception: essential considerations. *J Mot Behav.* 2012;44:403–18.
102. Maffioletti NA, Roig M, Karatzanos E, Nanas S. Neuromuscular electrical stimulation for preventing skeletal-muscle weakness and wasting in critically ill patients: a systematic review. *BMC Med.* 2013;11:137.
103. Ranck JBJ. Which elements are excited in electrical stimulation of mammalian central nervous system: a review. *Brain Res.* 1975;98:417–40.
104. Olsson H, Wessberg J, Morrison I, McGlone F, Vallbo Å. The neurophysiology of unmyelinated tactile afferents. *Neurosci Biobehav Rev.* 2010;34:185–91.
105. Griffin JW, George R, Ho T. Macrophage Systems in Peripheral Nerves. A Review *J Neuropathol Exp Neurol.* 1993;52:553–60.
106. Frostick SP, Yin Q, Kemp GJ. Schwann cells, neurotrophic factors, and peripheral nerve regeneration. *Microsurgery.* 1998;18:397–405.
107. Al-majed AA, Tam SL, Gordon T. Electrical stimulation accelerates and enhances expression of regeneration-associated genes in regenerating rat femoral Motoneurons. *Cell Mol Neurobiol.* 2004;24:379–402.
108. Tam SL, Gordon T. Mechanisms controlling axonal sprouting at the neuromuscular junction. *J Neurocytol.* 2003;32:961–74.
109. Tam SL, Gordon T. Neuromuscular activity impairs axonal sprouting in partially Denervated muscles by inhibiting bridge formation of Perisynaptic Schwann cells. *J Neurobiol.* 2003;57:221–34.
110. Geremia NM, Gordon T, Brushart TM, Al-majed AA, VMK V. Electrical stimulation promotes sensory neuron regeneration and growth-associated gene expression. *Exp. Neurol.* 2007;205:347–59.
111. Rockland KS. Axon collaterals and brain states. *Front Syst Neurosci.* 2018;12:32.
112. Varon SS, Bunge RP. Trophic mechanisms in the peripheral nervous system. *Annu Rev Neurosci.* 1978;1:327–61.
113. Agnew WF, McCreery DB, Yuen TGH, Bullara LA. Evolution and resolution of stimulation-induced axonal injury in peripheral nerve. *Muscle Nerve.* 1999; 22:1393–402.
114. Graczyk EL, Delhaye B, Schiefer MA, Bensmaia SJ, Tyler DJ. Sensory adaptation to electrical stimulation of the somatosensory nerves. *J Neural Eng.* 2018;15:046002.
115. Walker CF, Lockheed GR, Markle DR, McElhaney JH. Parameters of stimulation and perception in an artificial sensory feedback system. *J Bioeng.* 1977;1:251–6.
116. Anani AB, Körner LM. Afferent electrical nerve stimulation: human tracking performance relevant to prosthesis sensory feedback. *Med Biol Eng Comput.* 1979;36:1–4.
117. Vandoninck V, Van Balken MR, Agró EF, Petta F, Caltagirone C, Heesakkers JPF, et al. Posterior tibial nerve stimulation in the treatment of urge incontinence. *NeuroUrol Urodyn.* 2003;22:17–23.
118. Abdellaoui A, Préfaut C, Gouzi F, Couillard A, Coisy-Quivy M, Hugon G, et al. Skeletal muscle effects of electrostimulation after COPD exacerbation: a pilot study. *Eur Respir J.* 2011;38:781–8.

Ready to submit your research? Choose BMC and benefit from:

- fast, convenient online submission
- thorough peer review by experienced researchers in your field
- rapid publication on acceptance
- support for research data, including large and complex data types
- gold Open Access which fosters wider collaboration and increased citations
- maximum visibility for your research: over 100M website views per year

At BMC, research is always in progress.

Learn more biomedcentral.com/submissions

